

COPPER ADSORPTION USING PHOSPHORIC ACID-BASED GEOPOLYMERS

By

TEOH KHAY MIN

15097

Dissertation submitted in partial fulfillment of the requirements for

Bachelor of Engineering (Hons) Chemical Engineering

May 2014

Universiti Teknologi PETRONAS

Bandar Sri Iskandar

31750 Tronoh

Perak Darul Ridzuan

CERTIFICATION OF APPROVAL

Copper adsorption using phosphoric acid-based geopolymers

by

TEOH KHAY MIN

15097

A project dissertation submitted to the Chemical Engineering Programme
Universiti Teknologi PETRONAS in partial fulfillment of the requirement for the
BACHELOR OF ENGINEERING (HONS) CHEMICAL ENGINEERING

Approved by,

(PROF. DR. KHAIRUN AZIZI MOHD AZIZLI)

SUPERVISOR

UNIVERSITI TEKNOLOGI PETRONAS

TRONOH, PERAK

May 2014

CERTIFICATION OF ORIGINALITY

This is to certify that I am responsible for the work submitted in this project, that the original work is my own concept as specified in the references and acknowledgements, and that the original work contained herein have not been undertaken or done by unspecified sources or persons.

TEOH KHAY MIN

ACKNOWLEDGEMENT

First and foremost, I would like to thank God for His provision of strength and wisdom in finishing this Final Year Project.

I would also like to thank my supervisor, Prof. Khairun Azizi Mohd Azizli, who had been guiding me with patience and kindness, assisting me whenever there are any difficulties I faced throughout the entire period. Prof Khairun had been motivating me, encouraging me to march towards the completion of this project.

My heartfelt gratitude is extending to the following personnel who had contributed directly and indirectly towards this project:

Mr Irfan, postgraduate student in UTP who has been guiding me along side with Prof Khairun. Mr Irfan have be with me since the first day of this research, contributing ideas and explanations to findings in and out of this project.

En. Shaharuddin, En Asnizam, Cik Salmiyah, En Fadhullah Hakimi, En Fazli, En Shamsuddin and other technicians in Chemical Engineering, Petroleum Geoscience Department and Central Analysis Laboratory, for assisting me in equipments using and analysis process throughout the experimental works of this project.

Family members and friends who have been motivating me, supporting me and encouraging me, this project wouldn't be able to complete without the moral support from them.

ABSTRACT

Heavy metal pollution has been a recent topic and low cost adsorbents have been a trend to treat and remove heavy metals from waste water. The discovery of geopolymers has been a breakthrough in the field due to its amorphous and porous structure. The objectives of this research are to synthesize and characterize the phosphoric acid-based geopolymers using different phosphate to aluminum ratio. Raw material, kaolin was calcined to produce metakaolin which was then mix with phosphoric acid, distilled water and aluminum oxide powder to produce slurry geopolymer mixture. The mixture was cured at 80°C for 12 hours before it was being crushed, grounded and ball-milled into powder form. Different properties of geopolymers have been characterized, for instance, particle size, chemical composition, surface structure and porosity. The synthesized geopolymers, GP-1M and GP-2M were then utilized for adsorption test for removing copper ions. MIP study has shown that a larger pore volume is present in GP-1M (133.51mm³/g) as compared to GP-2M. The heavy metal removed was optimized at pH value of 6.5 for GP-1M. An increase of contact time also increases the percentage removal of copper ions by both geopolymers. The adsorption activities of both GP-1M and GP-2M fitted the pseudo first order reaction kinetic model at correlations coefficients value of 0.66 and 0.84. The adsorption studies also found to be fitted into Freundlich Isotherm with correlation coefficients of 0.998 and 0.728 respectively.

TABLE OF CONTENTS

CONTENT	PAGE
Certification of Approval	i
Certification of Originality	ii
Acknowledgement	iii
Abstract	iv
Table of Contents	v
List of Tables	viii
List of Figures	ix
Chapter 1: Introduction	
1.1 Background of Study	1
1.1.1 Introduction to heavy metals	1
1.1.2 Adsorption using geopolymers	2
1.2 Problem Statement	4
1.3 Objectives	5
1.4 Scope of Study	5
Chapter 2: Literature Review	
2.1 Introduction	6
2.2 Adsorption	7
2.2.1 Adsorption Theory	7
2.2.2 Type of Adsorptions	8
2.2.3 Type of Adsorbents	9
2.2.4 Equilibrium Relations for Adsorption	10
2.2.4.1 Linear Isotherm	11
2.2.4.2 Freundlich Isotherm	11
2.2.4.3 Langmuir Isotherm	11
2.2.5 Factors affecting Adsorption	12
2.3 Geopolymer	
2.3.1 Background of Geopolymer	13
2.3.2 Geopolymerization	14
2.3.2.1 Raw material and activator	15
2.3.3 Phosphoric Acid-based Geopolymers	16
2.3.4 Synthesis of Phosphoric Acid-based	17

	Geopolymers	
2.3.5	Adsorption using Geopolymers	17
2.4	Characterization and Analytical Techniques	19
2.4.1	Determination of Pore Size Distribution and Porosity	19
2.4.2	Analysis of Surface Structure	20
2.4.3	Determination of Particle Size	21
2.4.4	Determination of Chemical Composition and Functional Group	23
2.5	Determination of Copper Concentration	25
Chapter 3: Methodology		
3.1	Overview	26
3.2	Preparation and Characterization of Raw Material	27
3.3	Synthesis of Phosphoric Acid-based Geopolymers	27
3.4	Characterization of Phosphorus Acid-based Geopolymers	28
3.4.1	Determination of surface porosity	28
3.4.2	Determination of composition and functional groups	28
3.4.3	Study on surface structure	29
3.5	Adsorption Experiment	29
3.5.1	Effect of pH	29
3.5.2	Effect of contact time	30
3.5.3	Kinetic and Isotherm Study	30
Chapter 4: Results and Discussion		
4.1	Characterization of raw material	31
4.2	Characterization of geopolymers	31
4.2.1	XRF Analysis	32
4.2.2	FTIR Analysis	32
4.2.3	MIP Analysis	34
4.2.4	Particle Size Analysis (PSA)	35
4.2.5	FESEM Analysis	36
4.3	Initial adsorption experiment result	38

4.3.1	Effect of initial adsorbent dosage.	38
4.3.2	Effect of pH.	40
4.3.3	Kinetic Study	41
4.3.4	Isotherm Study	45
4.4	Adsorption Test Result	49
4.4.1	Effect of pH	49
4.4.2	Effect of contact time	50
4.4.3	Kinetic study of Adsorption	50
4.4.4	Isotherm Studies of Adsorption	54
Chapter 5: Conclusion and Recommendations		57
5.1	Conclusion	57
5.2	Recommendations	57
References		59

LIST OF TABLES

CONTENT	PAGE
Chapter 1: Introduction	
1.1 Literature works on heavy metal adsorption by geopolymers.	3
Chapter 2: Literature Review	
2.1 Parameters concentration limit for both Standard A and B.	7
2.2 Differences between physisorptions and chemisorptions.	9
2.3 Commercially used adsorbent and properties.	10
2.4 Result given by XRF on the composition of coal fly ash and fly ash-based geopolymer in term of weight percent	23
Chapter Three: Methodology	
3.1 Summary of components mass during synthesis of geopolymers.	21
3.2 Experiment design of adsorption experiment.	22
Chapter Four: Result and Discussion	
4.1 XRF result of kaolin and metakaolin	31
4.2 XRF result of GP-1M and GP-2M.	32
4.3 Comparison of k_1 , q_e and R^2 values of GP-1M and GP-2M for pseudo first order reaction model for methylene blue adsorption.	44
4.4 Comparison of k_2 , q_e and R^2 values of GP-1M and GP-2M for pseudo second order reaction model for methylene blue adsorption.	45
4.5 Values of Langmuir isotherm constants for GP-1M and GP-2M in methylene blue adsorption test.	48
4.6 Values of Freundlich isotherm constants for GP-1M and GP-2M in methylene blue adsorption test.	48
4.7 Comparison of k_1 , q_e and R^2 values of GP-1M and GP-2M for pseudo first order reaction model.	52
4.8 Comparison of k_2 , q_e and R^2 values of GP-1M and GP-2M for pseudo second order reaction model.	53
4.9 Values of Langmuir and Freundlich constants for GP-1M and GP-2M.	56

LIST OF FIGURES

CONTENT	PAGE
Chapter Two: Literature Review	
2.1 Mechanism of adsorption process.	8
2.2 Examples of adsorption isotherms.	11
2.3 Mechanism of geopolymerization.	15
2.4 Total water porosity of three different samples which were dried using four different method each as measured by MIP	20
2.5 Example of scanning image provides by SEM	21
2.6 Particle size distribution of natural pozzolan from Taftan Mountain.	22
2.7a FTIR result of geopolymers with different activators used and	24
2.7b curing conditions.	
Chapter Three: Methodology	
3.1 Summary of research methodology.	26
Chapter Four: Result and Discussion	
4.1 FTIR result of GP-1M.	33
4.2 FTIR result of GP-2M.	33
4.3 Pore size distribution of GP-1M.	34
4.4 Pore size distribution of GP-2M.	35
4.5 Particle size distribution curve of GP-1M.	36
4.6 Particle size distribution curve of GP-2M.	36
4.7 FESEM micrographs of GP-1M at 1,000, 5,000 and 10,000 magnification.	37
4.8 FESEM micrographs of GP-2M at 1,000, 5,000 and 10,000 magnification.	37
4.9 Effect of initial adsorbent dosage on methylene blue adsorption using GP-1M.	38
4.10 Effect of initial adsorbent dosage on methylene blue adsorption using GP-2M.	38
4.11 Effect of initial adsorbent dosage on methylene blue adsorption using GP-1M and GP-2M.	39
4.12 Effect of pH on adsorption of methylene blue using GP-1M.	40

4.13	Effect of pH on adsorption of methylene blue using GP-2M.	40
4.14	Effect of pH on the adsorption of methylene blue using GP-1M and GP-2M.	41
4.15	Pseudo first order kinetic model (GP-1M).	42
4.16	Pseudo first order kinetic model (GP-2M).	42
4.17	Pseudo second order kinetic model (GP-1M).	43
4.18	Pseudo second order kinetic model (GP-2M).	43
4.19	Langmuir isotherm (GP-1M).	45
4.20	Langmuir isotherm (GP-2M).	46
4.21	Freundlich isotherm (GP-1M).	46
4.22	Freundlich isotherm (GP-2M).	47
4.23	Effect of pH on Cu ²⁺ adsorption.	40
4.24	Effect of contact time	41
4.25	Pseudo first reaction model for GP-1M.	43
4.26	Pseudo first reaction model for GP-2M.	43
4.27	Pseudo second reaction model for GP-1M.	44
4.28	Pseudo second reaction model for GP-2M.	45
4.29	Langmuir Isotherm for GP-1M.	46
4.30	Langmuir Isotherm for GP-2M.	46
4.31	Freundlich Isotherm for GP-1M.	47
4.32	Freundlich Isotherm for GP-2M.	47

CHAPTER 1

INTRODUCTION

1.1. BACKGROUND OF STUDY

1.1.1. Introduction to heavy metals

Heavy metals are materials which have density of more than 5g/cm^3 (Barakat, 2010). The presence of heavy metals has significant impact to both the environment and human health, thus the concentration of heavy metals in water must be tightly controlled. There are various industries producing waste water that contains heavy metals such as printed circuit board manufacturing, metal finishing, automotive, aerospace, semiconductor and electroplated metal parts industry etc (Dissolved Metals Removal from Wastewater, 2014).

Copper is a popular material used in plating process in semiconductor industry. The used of copper in electroplating provide highly conductive surface for circuits. Other than that, copper wire is used as bonding wire in integrated circuits other than gold wire. Copper has several functions in human body and used in fixing connective tissue and calcium in bones, produce energy in cells, immune response, granular system, nervous system and reproductive system (Wilson, 2014). However, excessive ingestion of copper may cause vomiting, abdominal pain, diarrhea and discoloration of hair (Copper Poisoning, 2012). United State of Environmental Protection Agency (USEPA) also listed evidence that copper causes testicular cancer.

In Malaysia, according to Environmental Quality (Sewages and Industrial Effluents) Regulations 2009, Third Schedule, the permissible concentration of copper in waste water are 0.20mg/L and 1.0mg/L for Standard A and B respectively. However, a studies conducted by Ali et.al. in 2004 found out that the soil samples obtained from Mamut riverbank in Malaysia contain high amount of heavy metals. The results were presumed to be due to inappropriate waste management by mining activities nearby. Besides that, Fairchild Semiconductor (M) Sdn. Bhd., as a leading company in semiconductor industry which is based in Penang Island also provided a

report showing the high amount of copper (Cu), tin (Sn) and iron (Fe) in their untreated wastewater.

There are many processes and techniques been used to remove heavy metals in waste water. However, there are still disadvantages or drawbacks which motivate more research on relatively more sustainable and effective ways to treat the heavy metals contaminated wastewater. For instance, chemical precipitation produces excessive amount of sludge which brings environmental impact on its disposal while ion exchange cannot handle concentrated metal solution and corrosion become significant limiting factor for electrolytic recovery method (Barakat, 2010). Adsorption is another option in treating heavy metal containing waste water. Common adsorbent used in industry nowadays include activated carbons, zeolites and silica gel. Following the discovery of porous structure of geopolymers, geopolymers was also being studied on their adsorption capabilities of heavy metal.

1.1.2. Adsorption using geopolymers

Adsorption is a process normally adopted in the removal of heavy metals due to its low cost and promising efficiency. Adsorption is a mass transfer process whereby a substance is transferred from its original liquid phase to the surface of a solid, which is the adsorbent (Barakat, 2010). Many different materials such as industrial waste, natural materials and agricultural waste had been used in experiment to investigate their adsorption efficiency respectively.

Though there are different types of adsorbents being used in industry currently, there are still drawbacks on the adsorbents used, motivating the research and discovery of new adsorbent materials. For example, although activated carbon gives a large surface area to volume ratio, one of the disadvantages is its relatively high cost (Savova, et al., 2001). Besides that, cation-exchange resins also remain an expensive material to be used in industrial scale though the adsorbent provide effective heavy metal removal (Repo, Warchol, Kurniawan, & Sillanpaa, 2010). The used of chitosan-based adsorbent in wastewater treatment is impractical due to its inconsistent source and quality of chitin. The impracticality is also caused by the

difficulty in controlling the acetyl group distribution along the polymer backbone (Crini & Badot, 2008).

Geopolymers, synthesized using metakaolin or fly ashes which are rich in aluminosilicate, is a potential adsorbent material, due to its known amorphous porous structure, corrosion resistant, heat resistance and effective solidification of toxic waste (Cheng, Lee, Ko, Ueng, & Yang, 2012). Table 1.1 shows the summary of some literature works on the heavy metal adsorption by geopolymers.

TABLE 1.1- Literature works on heavy metal adsorption by geopolymers.

Year	Authors	Geopolymers used	Parameters tested	Heavy metals studied
2011	Kamel Al-Zboon, Mohammad S. Al-Harabsheh, Falah Bani Hani	Fly-ash based geopolymers Activator: Sodium hydroxide	Geopolymer dosage, lead initial concentration, contact time, pH and temperature	Lead ions
2012	T.W. Cheng, M.L. Lee, M.S. Ko, T.H. Ueng, S.F. Yang	Metakaolin-based geopolymers Activator: Sodium Hydroxide	Contact time, heavy metals initial concentration, pH and temperature.	Lead ions, copper ions, chromium ions, cadmium ions

There is another type of geopolymers, the phosphoric-acid geopolymers, which had been successfully synthesized and characterized (Liu, Cui, Qiu, Yu, & Zhang, 2010). However, existing literature on the adsorption of heavy metals using phosphoric-acid geopolymers is scant.

1.2. PROBLEM STATEMENT

The removal of copper ions from waste water is essential to ensure the sustainability of our balanced ecosystem and healthy environment. However, existing ways of removing heavy metals such as chemical precipitation, ion exchange etc. have their own limitations which include low loading rate, sludge formation. Adsorption using geopolymers definitely has high potential to replace current ways of removing heavy metals due to its proven high porosity, high tensile strength, thermally stable and corrosion resistant properties.

Phosphoric acid-based geopolymers is the one of the acid based geopolymers being synthesized which had similar properties as other alkaline-based geopolymers such as metakaolin-based geopolymers and fly ash-based geopolymers. There had been studies on fly ash-based geopolymers and metakaolin-based geopolymers, proving the heavy metals adsorption capabilities of respective geopolymers due to their porous structure.

Though there has been no report on the adsorption capabilities of phosphoric acid-based geopolymers, due to the similar properties with alkaline-based geopolymers and even superior performance with good mechanical and thermal properties, phosphoric acid geopolymers has great potential to provide a better heavy metal removal efficiency.

This project will focus on phosphoric acid-based geopolymers effectiveness in removing copper ions in wastewater. Understanding that different operating conditions bring different effect on adsorption process (Barakat, 2010), this research project will also investigate the effects of pH and temperature on the effectiveness of copper ions removal in wastewater.

1.3. OBJECTIVES

The objectives of this research project are

1. To synthesize phosphoric acid-based geopolymers by altering the phosphorus to aluminum ratio at ambient temperature.
2. To characterize geopolymers formed in terms of porosity, surface structure, composition and particle size using various analytical tools and techniques.
3. To study the effect of pH and contact on copper ions removal efficiency by phosphoric acid-based geopolymers.
4. To study the kinetic model and isotherms of adsorption activities exhibited by phosphoric acid-based geopolymer.

1.4. SCOPE OF STUDY

This research work scope will focus on the use of phosphoric acid-based geopolymers as adsorbent in copper ions removal. Different samples of phosphoric acid-based geopolymer will be synthesized using different aluminum to phosphate ratio. Metakaolin will be mixed at ambient temperature with distilled water, aluminum oxide and phosphoric acid under specific ratio before the slurry mixture is being placed in oven to be cured for 5 hours at 80°C. Characterization of geopolymers will be done using MIP to determine the porosity of the geopolymers, SEM to observe the surface structure of geopolymers and PSA to identify the particle size. The composition of geopolymers will also be determined using XRF and FTIR.

The phosphoric acid-based geopolymers will be used in copper ions adsorption test at various pH and temperature.

CHAPTER 2

LITERATURE REVIEW

2.1. INTRODUCTION

Heavy metals are materials which has density of more than 5g/cm^3 (Barakat, 2010). Some examples of heavy metal are arsenic (As), cadmium (Cd), zinc (Zn), chromium (Cr), copper (Cu), nickel (Ni), lead (Pb) and mercury (Hg). Due to its significant negative impact to both environment and human health, concentration of heavy metal in wastewater had been controlled tightly all around the world.

According to Environmental Quality (Sewage and Industrial Effluents) Regulations, 1979 in Malaysia, the industrial effluents quality can be divided into two standards, Standard A which is applied to inland waters within catchment areas mentioned in Fourth Schedule in the same regulation and Standard B which applies to other inland waters. Table 2.1 shows the limit of all parameters concentration limit for both Standard A and B in Environmental Quality (Sewage and Industrial Effluents) Regulations, 1979.

For an electronic industry, due to different operations in the production line such as electroplating, coating, electroless depositions, milling etc., heavy metals may diffuse into water in a hazardous level. Other than copper, wastewater from electronic industry also contains lead, nickel, tin, zinc and iron. It is very essential to keep the amount of these heavy metals way below the permissible concentration limit as to avoid leakage of heavy metals to free water and poison the marine ecosystem. There are a lot of different ways in removing heavy metals from industrial effluents and one of the most adopted methods is adsorption (Barakat, 2010).

TABLE 2.1- Parameters concentration limit for both Standard A and B.

Parameter	Unit	Standard A	Standard B
Temperature	°C	40	40
pH value	-	6.0-9.0	5.5-9.0
BOD5 at 20°C	mg/L	20	50
COD	mg/L	50	100
Suspended Solids	mg/L	50	100
Mercury	mg/L	0.005	0.05
Cadmium	mg/L	0.01	0.02
Chromium, hexavalent	mg/L	0.05	0.05
Arsenic	mg/L	0.05	0.10
Cyanide	mg/L	0.05	0.10
Lead	mg/L	0.10	0.5
Chromium, trivalent	mg/L	0.20	1.0
Copper	mg/L	0.20	1.0
Manganese	mg/L	0.20	1.0
Nickel	mg/L	0.20	1.0
Tin	mg/L	0.20	1.0
Zinc	mg/L	1.0	1.0
Boron	mg/L	1.0	4.0
Iron (Fe)	mg/L	1.0	5.0
Phenol	mg/L	0.001	1.0
Free Chlorine	mg/L	1.0	2.0
Sulphide	mg/L	0.5	0.50
Oil and Grease	mg/L	Not detectable	10.0

2.2. ADSORPTION

2.2.1. Adsorption Theory

Adsorption is one of the separation methods where components of fluids are adsorbed onto surface of solids which we call the adsorbent (Geankoplis, 2003). When the adsorbent become saturated with the solute (desired components to be

removed), the adsorbent will be regenerated by acid-wash or water-wash. Different from absorption process which occurs throughout the whole volume, adsorption only occurs at the surface of the particles. According to Figure 2.1, the mechanism of adsorption process can be explained in three steps which is diffusion, migration and adsorption process.

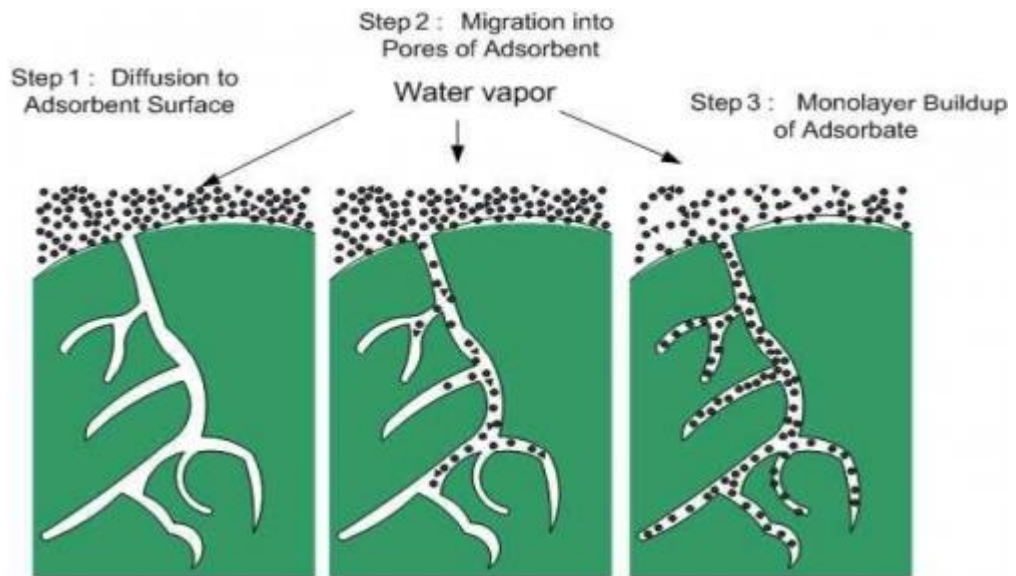


FIGURE 2.1- Mechanism of adsorption process (Kim & Chea, 2012).

The adsorbates which are the particles in the solvent will diffuse to the surface of adsorbent. Then the adsorbates will migrate into the porous structure of adsorbent. Finally, the adsorbates will be adsorbed to the surface of adsorbent.

2.2.2. Type of Adsorptions

There are basically two type of adsorption process, physical adsorption (physisorptions) and chemical adsorption (chemisorptions). Physisorption is a type of adsorption in which the adsorbates is adsorbed on the surface of adsorbents only through Van der Waals force, while chemisorption happens when adsorbates adhere to the adsorbent though the formation of chemical bonds. The type of adsorption that occurs simply depends on the types of adsorbate involved and their respective reaction with adsorbent. Table 2.2 summarizes the differences between physisorption and chemisorption.

TABLE 2.2- Differences between physisorptions and chemisorptions.

Physisorption	Chemisorption
Van der Waals force of attractions between adsorbent and adsorbate.	Chemical bonds formed between adsorbate and adsorbent.
Low enthalpy of adsorption (20-40 kJ/mole)	High enthalpy of adsorption (200-400kJ/mole)
Process occurs under low temperature.	Process takes place at high temperature.
Process is not specific.	Process is highly specific.
Multi-molecular layers adsorption may be formed.	Monomolecular layer adsorption is formed.
Process is reversible.	Process is irreversible.

(Jaan, 2012) (Geankoplis, 2003)

2.2.3. Type of Adsorbents

Adsorbents are materials which are porous in structure and have pore volumes of up to 50% of total particle volume (Geankoplis, 2003). Normally an adsorbent is in the form of small particles, pellets, beads or granules sized from 0.1mm to 12mm. They are often being used as packing beds in adsorption column. Table 2.3 lists the commercially used adsorbent and their respective properties.

Nevertheless, scientists continuously work on the development of adsorbents by using various raw materials such as agricultural waste, industrial by-products, natural materials and modified biopolymers (Barakat, 2010). The development of new adsorbent species is due to the discovery of raw materials with lower cost yet higher adsorption capacities. For instance, modified natural materials such as calcined phosphate, activated phosphate and zirconium phosphate had been proven to have much higher lead ions removal compared to zeolite.

Besides that, industrial waste such as fly ashes, waste iron, iron slags and hydrous titanium oxide also been studied to exhibit adsorbent properties. These industrial by-products are chemically modified to be used as adsorbent in heavy metal removal process from waste water. The development of industrial waste-based

adsorbent is sustainable, low cost and effective and hence makes them a popular option for adsorbent materials.

TABLE 2.3- Commercially used adsorbent and properties.

Adsorbents	Properties
Activated carbon	-Microcrystalline structure -Surface area of 300-1200m ² /g -Average pore diameter of 10-60Å
Silica gel	-Surface area of 600-800m ² /g -Average pore diameter of 20-50Å -Used to dehydrate gases and liquids and to fractionate hydrocarbons.
Activated alumina	-Surface area of 200-500m ² /g -Average pore size of 20-140Å -Used to dry gases and liquids
Molecular sieve zeolites	-Porous crystalline aluminosilicates -Open crystal lattice contain precisely uniform pores -Average pore size 3-10Å -Used for drying, separation of hydrocarbons and mixtures.
Synthetic polymers/resins	-Used to adsorb non-polar organics from aqueous solution.

(Geankoplis, 2003)

2.2.4. Equilibrium Relations for Adsorption

There is an equilibrium relationship between the adsorbent concentration and adsorbate concentration in adsorption process. Both of the parameters can be related using three isotherms as plotted in Figure 2.2.

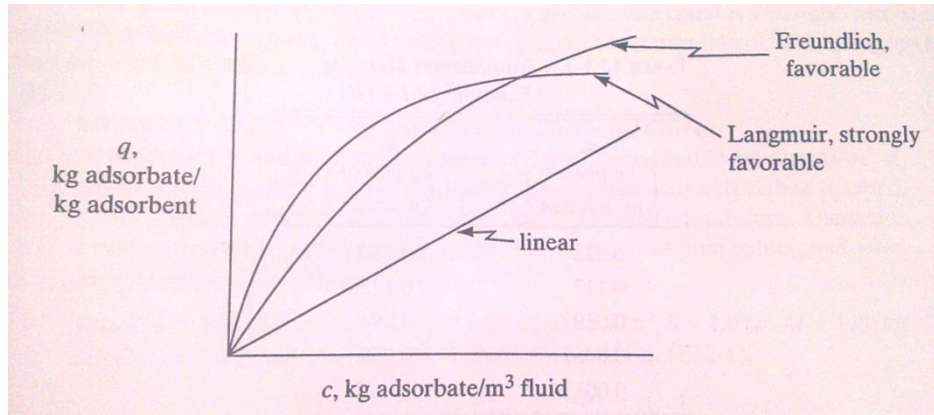


FIGURE 2.2- Examples of adsorption isotherms.

2.2.4.1. Linear Isotherm

From Figure 2.2, the first isotherm which defines the relationships between q (kg adsorbate/kg adsorbent) and c (kg adsorbate/m³ fluid) is the linear isotherm. The relationship also can be expressed using Equation 2.1.

$$q = Kc \quad (2.1)$$

Where K is the constant expressed in m³/kg adsorbent. Although the linear isotherm is not common in the entire adsorption process, but it can applied for dilute region in adsorption process to determine data for many systems.

2.2.4.2. Freundlich Isotherm

The Freundlich isotherm is mostly applicable to physical adsorption and useful for liquid system. Equation 2.2 shows the correlation of q and c in an equation form.

$$q = Kc^n \quad (2.2)$$

The value of K and n can be determined graphically, providing a series of q and c value determined through experiment.

$$\log q = \log K + n \log c \quad (2.3)$$

By plotting the graph of $\log q$ against $\log c$, the slope of the graph will be the value of n while the y-intercept of the graph will be the logarithm value of K according to Equation 2.3.

2.2.4.3. Langmuir Isotherm

The Langmuir isotherm is the strongly favorable type of isotherm for an adsorption process. Equation 2.4 shows the relationship between q and c in Langmuir isotherm.

$$q = \frac{q_0 c}{K + c} \quad (2.4)$$

q_0 is expressed as kg of adsorbate/kg solid while K is kg/m^3 . The equation is applied with assumption of monolayer adsorption, active sites on adsorbent are fixed, adsorption reached equilibrium and adsorption process is reversible. The value of q_0 and K can be determined by plotting graph of $1/q$ versus $1/c$ according to Equation 2.5.

$$\frac{1}{q} = \frac{K + c}{q_0 c} = \frac{K}{q_0} \left(\frac{1}{c}\right) + \frac{1}{q_0} \quad (2.5)$$

Where the slope is K/q_0 and intercept is $1/q_0$ (Geankoplis, 2003).

2.2.5. Factors affecting Adsorption

There are a number of factors which affect the adsorption process other than the qualities of adsorbent itself which includes dosage of adsorbents, pH, temperature, contact time and initial concentration of adsorbates (Al-Zboon, Al-Harabsheh, & Hani, 2011).

The rate of adsorption increases with the increase of dosage of adsorbents as more adsorbents provide more binding site for adsorbates. However, the cost of adsorbents is to be considered in order to achieve balance between removal efficiency and cost optimization.

In a study conducted by Al-Zboon. K. et al. (2011), the adsorption process increase as the temperature increases from 25 to 45°C. However, as an exothermic process, almost all adsorption process shows a decrease in adsorption rates as temperature increase (Geankoplis, 2003). This is due to the heat energy which excites the adsorbates molecules, breaking their weak Van der Waals interactions

with the adsorbent. The observation is very useful as desorptions can be achieved by increasing the temperature during backwashing.

Influence of pH on adsorption process can be explained through the presence of hydrogen ions and hydroxide ions in the solution. Past research works had shown a significant increase of adsorption rate with the increase of pH from 1-5 (Cheng, Lee, Ko, Ueng, & Yang, 2012) (Al-Zboon, Al-Harashseh, & Hani, 2011). This is due to the large amount of hydrogen ions (H^+) in the solution, creating a competing environment for adsorbate to bind to the adsorbent. However, the optimum pH of adsorption of different adsorbate again depends on the species of the desired adsorbate (Al-Zboon, Al-Harashseh, & Hani, 2011).

The equilibrium contact time of adsorption is dependent on the species of adsorbate studied. For example, studies showed that the equilibrium contact time for lead ions adsorption was 60min. Al-Zboon et al. (2011) experiments of investigating the effect of contact time by using fly ash-based geopolymers in adsorption process observed that the significant removal of lead ions occurs in the first 30 min and reached 80.24% of removal. As the contact time is prolonged to 120 min, the total removal of lead ions reached 91% and remains constant after that.

Due to the limiting binding sites presence in adsorbent, the increase of adsorbate initial concentration might result in lower percentage of removal and consequently the efficiency (Al-Zboon, Al-Harashseh, & Hani, 2011).

2.3. GEOPOLYMER

2.3.1. Background of Geopolymer

History of geopolymers can be traced back to late 1970s, developed by Davidovits, J.. Geopolymers are materials which is made up of polymeric Si-O-Al functional group, creating a framework similar to zeolites, but more amorphous instead of crystalline. There are small aluminosilicate clusters with dispersed pores within a highly porous network (Huang & Han, 2011). Geopolymers have been used up for many applications. One of the major applications of geopolymers is in the construction industry. This is due to its quick curing time and high tensile strength. Geopolymers' high thermal stability and corrosion resistant properties also make

them a superior option compare to other cement. Lastly, geopolymer manufacturing process which produces less carbon dioxide also make them a sustainable materials for the world (Davidovits, Geopolymer Cement, 2013). Other applications of geopolymers include archaeology and heavy metal adsorption.

Geopolymers can be synthesized easily under normal ambient condition using different raw materials, for instance fly ash and metakaolin. Fly ashes are waste products from the combustion process, released from thermal power plants and factories while metakaolin are simply heated kaolin which is also known as china clay. Both raw materials have high aluminosilicate content and highly favorable for the synthesis of geopolymers.

2.3.2. Geopolymerization

Geopolymer can be formed through geopolymerization. According to Ho (2012), geopolymerization is a geo-synthesis reaction between raw material of high alumino silicate content and alkaline solution which act as an activator. However, research has shown that other than alkaline solution, acidic solution also has been used as activator in geopolymerization process (Liu, Cui, Qiu, Yu, & Zhang, 2010).

The mechanism of geopolymerization can be summarized in Figure 2.3. Basically geopolymerization is separated into three stages. First stage is the formation of precursors, followed by orientation and internal restructuring of precursors and finally, the re-precipitation process which formed geopolymer (Al-Zboon, Al-Harashseh, & Hani, 2011). At the first stage, alkaline or acidic hydrolysis dissolve raw materials which are high in alumina and silica content and introduce aluminate and silicate species into the solution. Those units will then form larger and more complex precursors units by sharing oxygen atom in the second stage (Al-Zboon, Al-Harashseh, & Hani, 2011). As the reaction carries on, gelation occurs by condensation. The time needed for gel to form from the supersaturated solution will depends on several factors such as the processing condition of raw materials, the composition of solution and also the conditions of synthesis process (Ho, Geopolymer-based Coating Material for Metal Substrate, 2012). However, due to quick reaction between raw materials and activators in geopolymerization, the gel

formed will not have sufficient time to grow into a well crystallized-structure. The short and hardening and settling time results in a tightly packed polycrystalline structure which has unique properties. As gelation continues, the alumina-silicate network continues to increase in size and precipitate. Finally, geopolymers are formed in stage three after hardening.

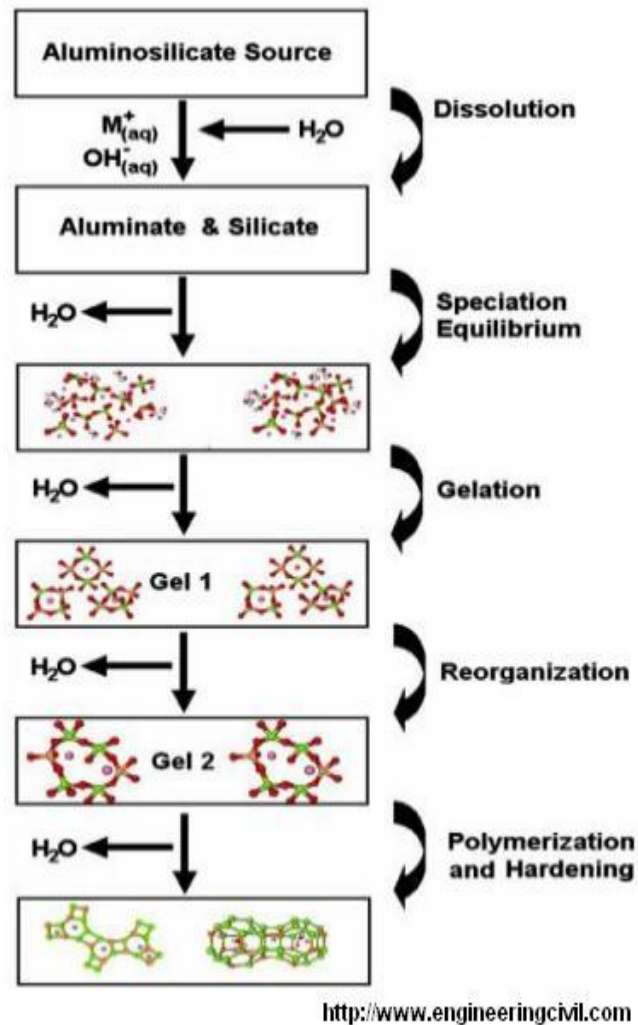


FIGURE 2.3- Mechanism of geopolymerization (Ho, Geopolymer-based Coating Material for Metal Substrate, 2012).

2.3.2.1. Raw material and activator

The most commonly used raw material for geopolymerization would be metakaolin and fly ash. Besides that, materials which are rich in aluminum and silica

are also being used as raw material for geopolymerization. For instance, clays, slag, silica fume, rice husk ash, red mud etc (Vijaya Rangan, 2010).

Fly ash contains high weight percent of silica and aluminum which are present in their oxides form. XRF analysis shows that typical coal fly ash would contain 50.73% of silica oxide and 28.87% of aluminum oxide (Al-Zboon, Al-Harashseh, & Hani, 2011). The silica oxide and aluminum oxide weight percent in metakaolin also reaches almost similar high concentration of 41.5% and 19.6% respectively (Cheng, Lee, Ko, Ueng, & Yang, 2012). The aluminum and silica content within the raw material is very essential and responsible in the formation of polymeric precursors ($-\text{SiO}_4-\text{AlO}_4-$, $-\text{SiO}_4-\text{AlO}_4-\text{SiO}_4-$) with the activators by sharing oxygen atoms. Ultimately, re-precipitation occurs to form geopolymers.

Activator is another important element in Geopolymerization. Activators are present in the process to balance the negative charge of aluminum (Al-Zboon, Al-Harashseh, & Hani, 2011). A commonly used activator in geopolymerization is alkaline solution such as sodium hydroxide or potassium hydroxide solution. However, metakaolin and fly ash can also be activated by acidic solution such as phosphoric acid (Douiri, Louati, Baklouti, Arous, & Fakhfakh, 2014) (Liu, Cui, Qiu, Yu, & Zhang, 2010) (Sadangi, Muduli, Nayak, & Mishra, 2013). For phosphoric acid-based geopolymer, reaction occurs between acid phosphate and metal oxide where silica ions are partially or totally being replaced by phosphate ions in the phosphoric acid.

2.3.3. Phosphorus Acid-based Geopolymers

Phosphoric acid-based geopolymers are slightly different from other alkaline-based geopolymers (metakaolin-based and fly ash-based). This is due to the addition of phosphoric acid solution during the synthesis process, causing a different polymeric linkage being formed between silica, aluminum and phosphorus. With the addition of phosphoric acid into the reaction, different polymeric linkages ($-\text{P-O-P-O-}$, $-\text{Al-O-P-O-}$ and $-\text{Si-O-Si-O-}$) are formed (What is geopolymer? Introduction, 2013).

Study by Liu, L. et al. (2010) shows that phosphorus acid-based geopolymers formed are amorphous, porous and displayed excellent thermal stability. Though there isn't any research has been done on the application of phosphoric acid-based geopolymers, the proven porous properties have made them a potential adsorbent material.

2.3.4. Synthesis of Phosphorus Acid-based Geopolymers

According to Liu, L. et al.(2010), the synthesis of phosphoric acid-based geopolymers can be done by adding phosphoric acid to the mixture of metakaolin and α -Al₂O₃ at ambient temperature. Metal powders (Al or Fe) will also be added as a pore forming agents. However, studies have also shown that by altering the components ratio, the geopolymers formed will possess different properties.

For instance, the amount of metal powder added affects the compressive strength and porosity of the geopolymers formed. High aluminum powder weight percentage will increase the porosity of the phosphoric acid-based geopolymers, but at the same time decreasing their compressive strength (Liu, Cui, Qiu, Yu, & Zhang, 2010). The same study also shows that low water content result in higher viscosity and smaller pore size. However, the products' compressive strength remains constant despite of elevated temperature from 80°C to 1450°C.

2.3.5. Adsorption using Geopolymers

Geopolymer had been studied and exhibit the quality to be an effective adsorbent due to its porous structure. In fact, there had been research works going on to examine the adsorption capabilities of geopolymers.

Fly ash-geopolymers are developed using industrial by-products, fly ash. Fly ashes contain high quantities of aluminosilicate, low cost and abundant in amount make them easily available to be used for the synthesis of geopolymers. The chemical modification of fly ashes into fly ash-based geopolymers is to create the amorphous structure in geopolymers, providing better adsorption efficiency. Fly ash-based geopolymers had been used to test its lead ion removal capabilities and the

results shown up to 90.6% of removal efficiency. Besides that, the same studies also investigate on the effects of different factors on the removal efficiency of lead ions by fly ash-based geopolymers. In conclusion of this study, the lead ions removal efficiency increase with the adsorbent dosage, contact time, temperature and the decrease of adsorbate initial concentration. The optimum pH for the adsorption process of lead ions is determined as 5 in this experiment study (Al-Zboon, Al-Harashseh, & Hani, 2011).

Another study by Cheng. T.W., (2012) was working on the heavy metal adsorption by metakaolin-based geopolymer. Instead of using fly ash as raw material, metakaolin was used in this research study. Metakaolin are commonly known as China clay and geopolymers formed contained high weight percent of silicon dioxide (41.5%) and aluminum oxide (19.6%). The same study also observes the increase of surface area from 50.9 m²/g to 65.7 m²/g after water and steam treatment and hence the author suggested that water and steam actually causing the water to wash and remove any debris present in the geopolymer structure. There are four different heavy metal ions involve in the studies that include lead ions, cadmium ions, copper ions and chromium ions. Result of the research shows excellent removal efficiency at pH 4 with highest removal efficiency of lead ions, followed by cadmium ions, copper ions and chromium ions. Other than that, the effects of pH and temperature were also studied in this experiment. The pH value of solution varies from 2 to 5 in the experiment and results shown an increase of removal efficiency as pH increase. However, the temperature study shows that the removal efficiency only increase slightly with the increase of temperature from 15 to 45°C (Cheng, Lee, Ko, Ueng, & Yang, 2012).

On the other hand, there aren't any study had been done on the heavy metal removal efficiency of phosphoric acid-based geopolymers. Although phosphoric acid-based geopolymers exhibit qualities as adsorbent, the effects of acidic based on heavy metal removal are yet to be investigated. Hence the main focus of this research work will be on the lead ions removal efficiency of this new material, phosphoric acid-based geopolymer.

2.4. CHARACTERIZATION AND ANALYTICAL TECHNIQUES

There are various analytical techniques being adopted in this research. Several tests and analysis had been carried out on geopolymers to determine the surface structure, porosity, particle size and composition using various tools. Besides that, Atomic Absorption Spectroscopy (AAS) technique is being applied to determine the copper concentration in solution before and after the adsorption test.

2.4.1. Determination of Pore Size Distribution and Porosity

The technique which will be adopted for this analysis will be Mercury Intrusion Porosimetry (MIP). MIP is a commonly used technique in the analysis and characterization of cement-based materials (Abell, Willis, & Lange, 1999). MIP is most often used to determine the pore size distribution, percent porosity, bulk and skeletal densities of a material (DeSousa & Webb, 2010). MIP works in the principle by intruding mercury into a material under high pressure with the use of a porosimeter. The commonly used of MIP is due to its simplicity. However, there are still some drawbacks in this technique which cause inaccurate results. For example, MIP is unable to accurately present exact pore size distribution of a material due to “ink bottle” effect (Abell, Willis, & Lange, 1999). “Ink bottle” effect is expected when MIP misinterpret the exact pore size according to their throats as some large pores are only accessible by narrow throat. Besides that, different drying methods give different results in MIP.

Research shows that sample preparation using different drying method gives different total water porosity in MIP. Figure 2.4 shows a bar chart plotted to compare the total water porosity measured by MIP using samples dried using different methods.

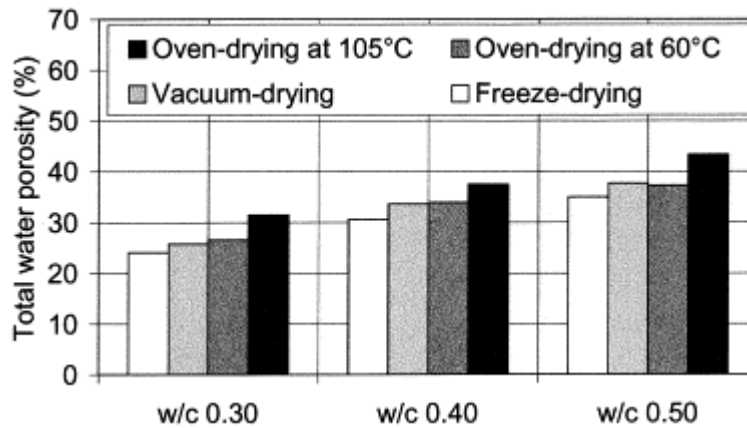


FIGURE 2.4- Total water porosity of three different samples which were dried using four different method each as measured by MIP (Gallé, 2001).

Figure 2.4 clearly shows higher total water porosity was measured by MIP if the samples were oven-dried at 105°C. However, the same research conducted by Gallé (2011) explained that at 105°C, the hydrated cement has been partly dehydrated; which cause differences in structure and the values of total water porosity obtained are overestimated.

2.4.2. Analysis of Surface Structure

The surface structure of phosphoric acid-based geopolymers is determined using Scanning Electron Microscope (SEM). SEM is a microscope which will give image of sample by scanning it with beam of electron. Electron beam will react with elements in the sample, producing signals which contain the information on the topography and composition of the sample. SEM is able to provide image with very high resolution, revealing details even to less than 1nm in size. Figure 2.5 shows an example of SEM generated image of a solid sample.

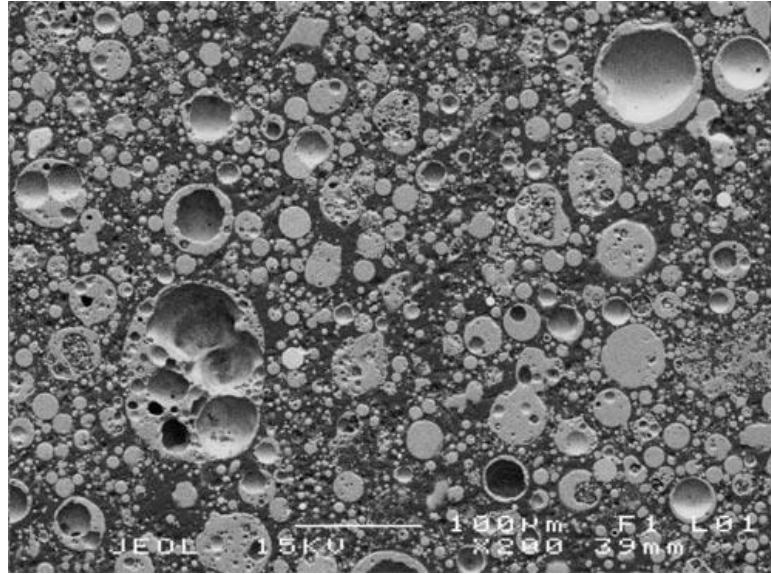


FIGURE 2.5- Example of scanning image provides by SEM (Geopolymer Research).

SEM utilizes vacuum conditions and electron beam to form images of samples. Hence, to prepare sample for SEM, water content in samples must first be removed to avoid vaporization in vacuum. Non-metal samples have to be made conductive by coating a thin layer of conductive material such as gold or palladium (Scanning Electron Microscope, 2014) (Liu, Cui, Qiu, Yu, & Zhang, 2010).

2.4.3. Determination of Particle Size

PSA is used to determine the size of a particulate solid. A PSA is expected to give results of volume of particulates with respect to their size range and one of the commonly used PSA in analytical industry would be Malvern Mastersizer 2000 Particle Size Analyzer.

Malvern Mastersizer 2000 is able to analyze both wet and dry sample using different dispersion units. Malvern Mastersizer 2000 operates using laser diffraction technique where intensity of laser light is detected by detectors after passes through the dispersed sample particles. The scattering pattern is able to calculate the size of particles after data analysis (Mastersizer 2000).

A typical PSA system consists of three elements which are sample dispersion units, optical bench and software program. Sample dispersion unit is a segregated

2.4.4. Determination of Chemical Composition and Functional Group

XRF are normally used for elemental analysis and chemical analysis to investigate building materials, metals, glasses and ceramics. XRF works in a way where X-ray is being emitted from source to the sample, ionizing the components atom. This ionization cause the atom structure to become unstable and electron at higher orbital level will fall to fill in the empty gap which is escaping electron left behind. During this “falling” process, energy is being released in the form of photon. Hence, XRF detects this type of radiation which is specific and special to each type of material, characterize the identity of element within sample.

Figure 2.7 shows a sample result given by XRF on the composition of raw fly ash and fly ash-based geopolymers. The weight percent of silicon oxide and aluminum oxide present in the fly ash decrease significantly as observed in Table 2.4. This is due to the addition of sodium hydroxide which causes the increase in content of hydroxyl and sodium group in the structure of geopolymers (Al-Zboon, Al-Harashseh, & Hani, 2011).

TABLE 2.4– Result given by XRF on the composition of coal fly ash and fly ash-based geopolymer in term of weight percent (Al-Zboon, Al-Harashseh, & Hani, 2011).

Compound (%)	Raw Ash	After Geopolymerization
SiO ₂	50.73	39.90
Al ₂ O ₃	28.87	19.70
Fe ₂ O ₃	11.93	7.50
CaO	1.73	2.43
MgO	1.39	1.13
K ₂ O	0.74	1.08
Na ₂ O	0.30	11.72
TiO ₂	1.41	0.50
SO ₃	0.35	0.25
L.O.I	2.53	14.69

FTIR is also an important technique to identify functional group of a sample. In FTIR, infrared radiation is being emitted to the samples and similarly to other spectroscopy, part of the radiation will be absorbed by the samples while some will pass through the samples. The resulting infrared spectrum is able to identify the quality, consistency, identity of samples and the amount of components present in the samples (What is FT-IR?, 2001).

Figure 2.7 (a) and (b) show the FTIR result of a study conducted by Bakharev in 2005, who was researching on the geopolymerization using different activators and curing conditions. Figure 2.7 (a) shows the FTIR results of geopolymer formed with sodium hydroxide as activator while Figure 2.7 (b) shows the FTIR geopolymer result formed by using sodium silicate as activator. Four curves shown in each figure represent the FTIR result of fly ash and FTIR results of geopolymer which were cured at three different conditions.

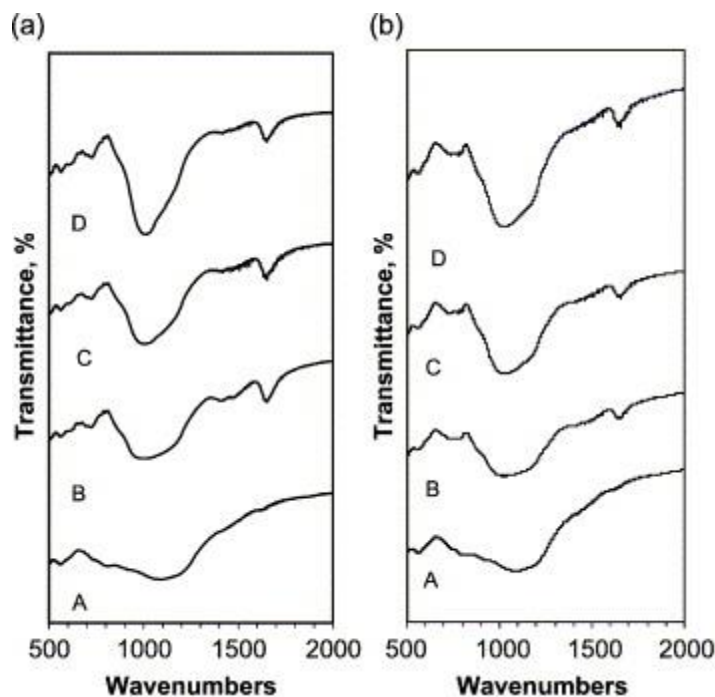


FIGURE 2.7 (a) and (b) - FTIR result of geopolymers with different activators used and curing conditions.

Curve A represents FTIR result of fly ash. Curve B is the result of geopolymer which was cured at 2 hours at room temperature, ramped to 95°C and heat cured at 95°C for 6 hours (Case III 95C). Curve C represents the geopolymer which was cured for 24 hours at room temperature, ramped to 75°C and heat cured at

75°C for 24 hours (Case II 75C). Curve D shows the FTIR result of geopolymer which was cured for 24 hours at room temperature, ramped to 95°C and heat cured at 95°C for 24 hours (Case II 95C).

2.5. DETERMINATION OF COPPER CONCENTRATION

Atomic Absorption Spectroscopy (AAS) is used in this research work to determine the concentration of copper in its solution. Concentration of copper in the solution will be determined before and after adsorption test to investigate the adsorption capabilities of geopolymers. AAS has been a commonly used technique in determination of metal content in solution. For instance, in a research work title the synthesis of ferronickel slag-based geopolymers, AAS had been used to determine the metal concentration in the slag before synthesis of geopolymers is being done (Marangkos, Giannopoulou, & Panias, 2009). AAS also has been proven suitable for analysis of real samples in 2012 (Bagheri, Afkhami, Saber-Tehrani, & Khoshsafar, 2012). Research has been done to determine the metal concentration in different water samples such as tap water and petrochemical wastewater using Flame AAS and the results were compared with Inductively coupled Plasma Atomic Emission Spectroscopy (ICP-AES) using t-test method. Both results eventually shows no significant difference at $P=0.05$ (Bagheri, Afkhami, Saber-Tehrani, & Khoshsafar, 2012).

CHAPTER 3

METHODOLOGY

3.1. OVERVIEW

This research work was divided into five main stages which were the preparation of raw material, the characterization of raw material, the synthesis of geopolymer using different phosphorus to aluminum ratio, characterization of geopolymer formed and adsorption experiment under different pH and temperature. Figure 3.1 shows the summary of research methodology for this research project.

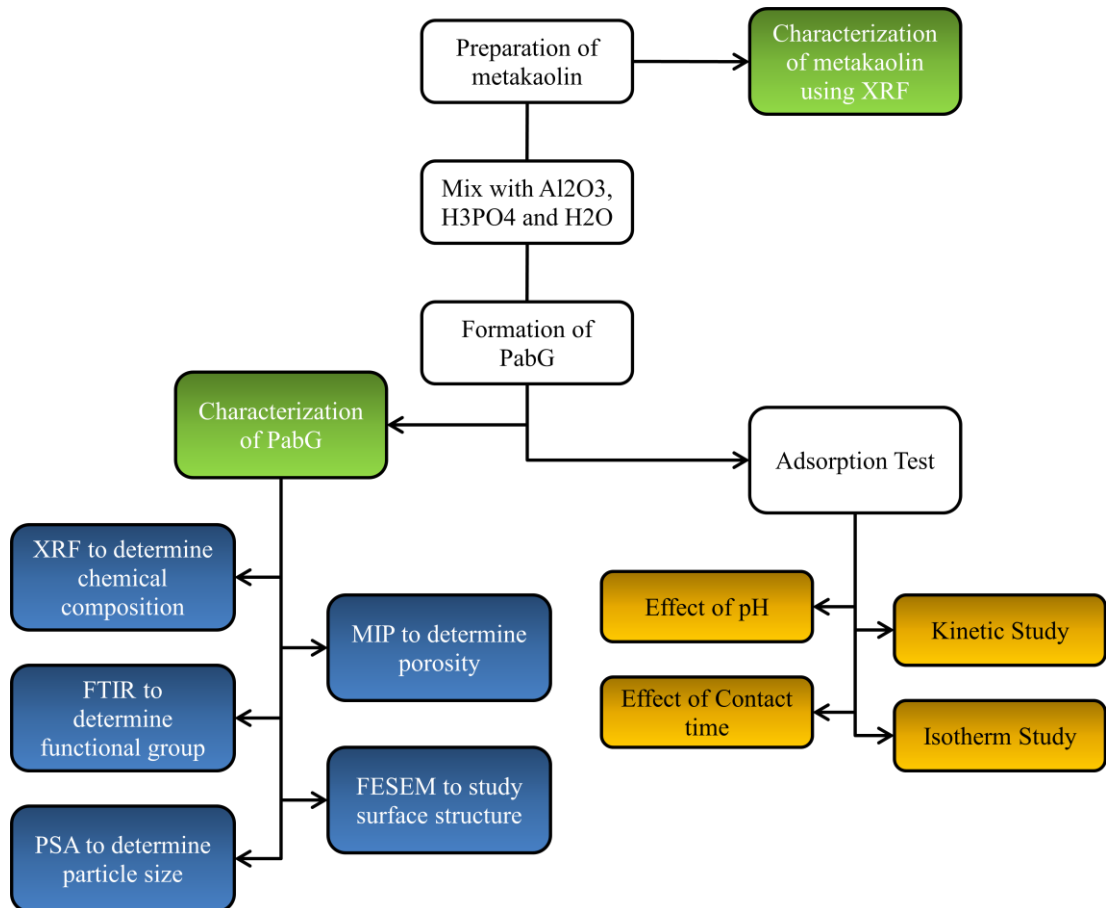


FIGURE 3.1- Summary of research methodology.

3.2. PREPARATION AND CHARACTERIZATION OF RAW MATERIAL

The raw material kaolin was calcined in the furnace at 800°C for 2 hours to form metakaolin before being used to synthesize phosphoric acid-based geopolymers. The composition of metakaolin formed was characterized using XRF. The characterization of metakaolin is essential to identify the amount of aluminum oxide added to form desired geopolymer.

3.3. SYNTHESIS OF PHOSPHORUS ACID-BASED GEOPOLYMERS

In this research, phosphoric acid-based geopolymers was used in the experiment. Method of synthesis was adopted from Liu et al. (2010). Geopolymers with different characteristics were synthesized with different phosphate to aluminum ratio. The synthesis process is summarized as below.

1. 50g of metakaolin was mixed with aluminum oxide powder, phosphoric acid solution and distilled water under ratio as summarized in Table 3.1.
2. The mixture was stirred thoroughly for 10 minutes and being poured in a plastic mould.
3. The mixture was then being cured at 80°C overnight.
4. The geopolymers formed with phosphate to aluminum ratio of 1:1 was labeled as GP-1M while the other was labeled GP-2M.
5. Geopolymers formed was then crushed and ball-milled.
6. Geopolymer powders were washed with distilled water thoroughly and dried at 105°C overnight in oven before being used for adsorption and characterization.

TABLE 3.1- Summary of components mass during synthesis of geopolymers.

Geopolymer	Metakaolin	Aluminum Oxide (Al ₂ O ₃)	Phosphoric acid (H ₃ PO ₄)	Distilled water
GP-1M	50g	38.82g	31.96cm ³	40cm ³
GP-2M	50g	38.82g	38.35cm ³	40cm ³

3.4. CHARACTERIZATION OF PHOSPHORUS ACID-BASED GEOPOLYMERS

3.4.1. Determination of surface porosity.

The surface porosity of respective geopolymers was determined through MIP. The process of characterization is listed below.

1. The geopolymer formed was crushed to size of no more than 8mm x 8mm x 10mm.
2. Sample selection was done by random pick.
3. The density and weight of samples were determined.
4. The sample was then being placed in the sample holder of MIP for analysis.

3.4.2. Determination of composition and functional groups

Composition of geopolymers was determined using XRF and FTIR.

1. Large portion of geopolymers was crushed and ball-milled.
2. The resulting geopolymer powder was further dried at 80°C for 5 hours.
3. Sample selection was done by coning and quartering until desired sample weight is obtained.
4. Sample powders were then kept inside transparent vials before being sent for analysis.
5. 3 g of each sample was mixed with 100 g of potassium bromide (KBr) powder prior to FTIR analysis.
6. The powder mixture was then being pressurized in hydraulic press at pressure of 15 tons.
7. The mixture disk was transferred to the disk holder of FTIR Spectrometer for analysis.

3.4.3. Study on surface structure.

The surface image of geopolymers was generated by SEM. Sample powders were first coated with a layer of conductive material in a sputter coater before being placed under the SEM for analysis.

3.5. ADSORPTION EXPERIMENT

The adsorption experiments were conducted using geopolymers synthesized as adsorbent while copper ion as adsorbate. pH and contact time will be the main parameters to be investigated in this research study. The adsorption experiment design is summarized in Table 3.2 below.

TABLE 3.2- Experiment design of adsorption experiment.

Investigated parameter	Initial copper concentration (ppm)	Temperature (°C)	pH	Contact time (min)
pH	8	25	3 5 7 9 10	180
Contact time	8	25	6.5	30 60 90 120 150 180

3.5.1. Effect of pH

As the pH of solution has a significant effect on the adsorption activities of adsorbents, the effect of pH on copper removal percentage is studied here in this research as well.

1. 25ml of 8ppm $\text{Cu}(\text{NO}_3)_2$ solution was added into 5 conical flasks.
2. The pH of solutions were measured and adjusted to 3, 5, 7, 9, 10 by adding 0.1M hydrochloric acid (HCl) or 0.1M sodium hydroxide (NaOH).

3. 0.4g of GP-1M powder was then measured, recorded and added into each of the conical flasks containing copper solution.
4. Water bath shaker was set to 25°C and shaking speed of 150 rpm.
5. Conical flasks were then immediately place into water bath shaker and timer was started.
6. A contact time of 3 hours is allowed for adsorption to occur.
7. Resulting solutions from conical flasks were obtained and being centrifuged to separate the copper solution from adsorbent.
8. Solutions obtained were analyzed using AAS.
9. The experiment was repeated using GP-2M.

3.5.2. Effect of contact time

Different adsorbent adsorb at different rate, a more effective adsorbent is able to adsorb more adsorbates and achieve equilibrium at a shorter contact time.

1. 50ml of 8ppm $\text{Cu}(\text{NO}_3)_2$ solution was added into a conical flask.
2. 0.8g of GP-1M powder was then measured, recorded and added into the conical flasks containing copper solution.
3. Water bath shaker was set to 25°C and shaking speed of 150 rpm.
4. Conical flasks were then immediately place into water bath shaker and timer was started.
5. A contact time of 3 hours is allowed for adsorption to occur.
6. 5 ml of solution was extracted at the interval of 30 minutes.
7. Solutions obtained were analyzed using AAS.
8. The experiment was repeated using GP-2M.

3.5.3. Kinetic and Isotherm Study

Experimental data obtained from the contact time experiment will be used to determine which kinetic model and isotherm that the adsorption activities of phosphoric acid-based geopolymers fitted into. The calculation process was aided with Microsoft Office Excel Spreadsheet.

CHAPTER FOUR

RESULTS AND DISCUSSION

4.1. CHARACTERIZATION OF RAW MATERIALS.

Metakaolin was produced through calcinations of kaolin at 800°C for 2hours. Table 4.1 shows the XRF results of both kaolin and metakaolin.

TABLE 4.1- XRF result of kaolin and metakaolin.

COMPONENTS	WEIGHT %	
	KAOLIN	METAKAOLIN
Al ₂ O ₃	37.7	38.9
SiO ₂	55.9	55.4
P ₂ O ₅	1.67	1.62
TiO ₂	1.76	1.65
Fe ₂ O ₃	1.74	1.47
CaO	0.46	0.431
K ₂ O	0.373	0.356
ZrO ₂	0.0247	0.0234
Ga ₂ O ₃	0.0122	0.0133
SO ₃	0.169	0.112
CuO	64.765ppm	91.458ppm
NiO	65.193ppm	-
Nb ₂ O ₅	85.348ppm	85.564ppm
MoO ₃	-	96.92ppm
Rb ₂ O	31.994ppm	34.659ppm
Ag	0.0101	-

The obtained result is close to previous research findings (Liu, Cui, Qiu, Yu, & Zhang, 2010) where metakaolin shows composition of 56.91 wt% SiO₂, 42.35 wt% of Al₂O₃, 0.22 wt% of Fe₂O₃ and 0.49 wt% of K₂O.

4.2. CHARACTERIZATION OF GEOPOLYMERS

There are two types of geopolymer being synthesized, labeled GP-1M and GP-2M. The particle size, composition, functional group, surface structure and

porosity of both geopolymers had been studied using different analytical tools and techniques. The characterization process is very essential for understanding of phosphoric acid-based geopolymers. Besides that, characterization of geopolymers will also help in relating the adsorption capabilities of geopolymers or even supporting it. The phosphoric geopolymers was characterized using XRF, FTIR, MIP, PSA and FESEM and details are discussed in sub-chapters below.

4.2.1. XRF Analysis

Compositions of geopolymers had been determined using XRF. Table 4.2 shows the components composition of GP-1M and GP-2M after XRF analysis.

TABLE 4.2- XRF result of GP-1M and GP-2M.

COMPONENTS	WEIGHT % in GP-1M	WEIGHT % in GP-2M
Al ₂ O ₃	36.5	34.2
SiO ₂	26	24.3
P ₂ O ₅	35.1	39.3
TiO ₂	0.75	0.718
Fe ₂ O ₃	0.746	0.693
CaO	0.463	0.432

There is an obvious increase of P₂O₅ content in GP-2M compared to GP-1M. The result is expected due to amount of phosphoric acid added during synthesis of GP-2M is 20% more than that of GP-1M. The composition of Al₂O₃ in both geopolymer is higher than that of SiO₂ as compared to metakaolin due to the addition of aluminum oxide (Al₂O₃) during the synthesis of geopolymer. A considerable increase of P₂O₅ in geopolymers as compared to metakaolin was observed due to the dissociation of phosphate ions which eventually bind themselves with oxygen atom. Phosphate bonded chemical activators was also proved to improve geopolymer compressive strength as compared to other activators (Sadangi, Muduli, Nayak, & Mishra, 2013).

4.2.2. FTIR Analysis

FTIR has been used to determine the functional group, stretch and bonding present in both GP-1M and GP-2M. Figures 4.1 and 4.2 show the FTIR results of GP-1M and GP-2M.

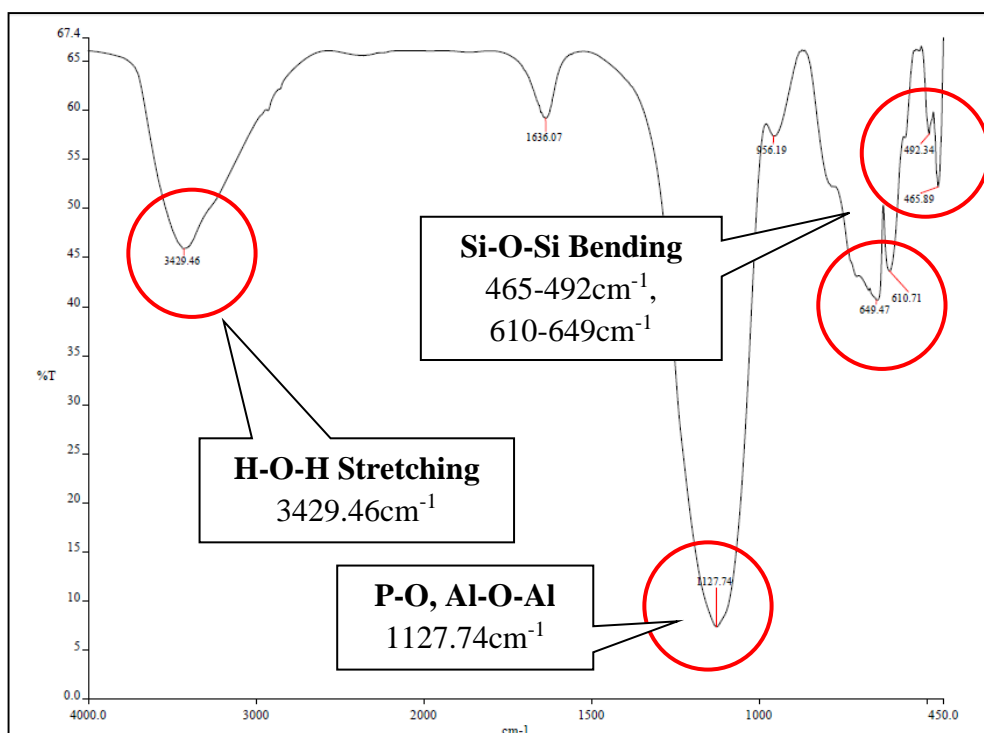


Figure 4.1- FTIR result of GP-1M.

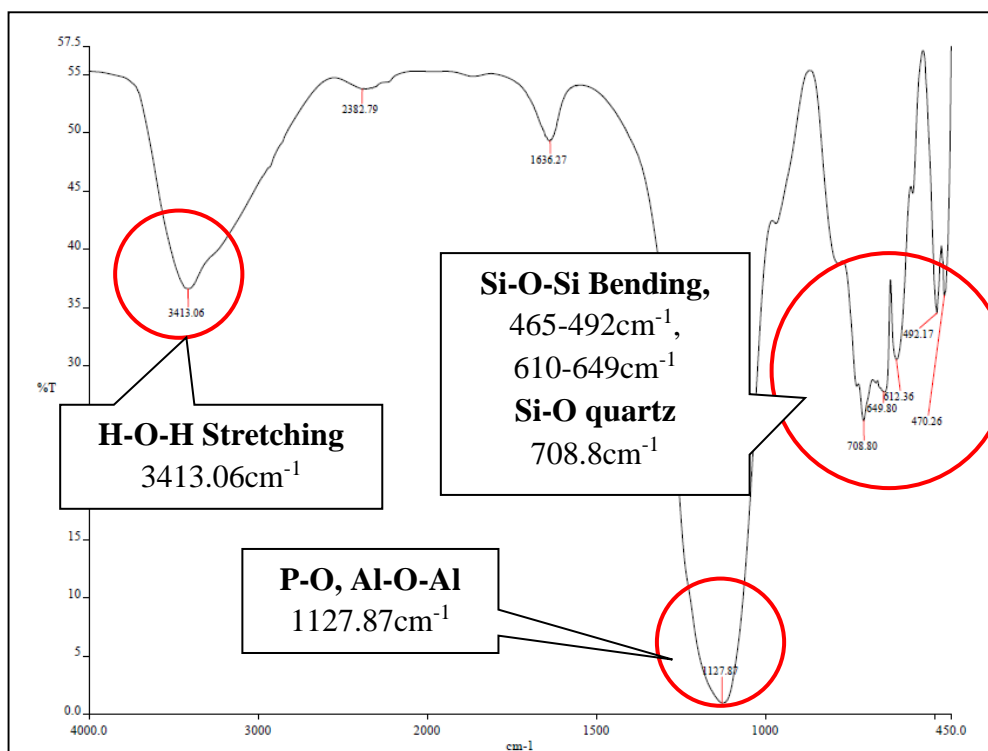


Figure 4.2- FTIR result of GP-2M.

Figure 4.1 and 4.2 shows important clues regarding the existence of geopolymerization in both GP-1M and GP-2M. Firstly, an obvious and strong peak

can be observed from both figures at the wavelength of 1127cm^{-1} , the peak actually correspond to the presence of P-O and Al-O-Al stretch in both geopolymers (Reusch, 2013). The observations are the results of geopolymerization and curing which transform the original amorphous structure to crystalline quartz (SiO_2) and berlinite (AlPO_4) (Liu, Cui, Qiu, Yu, & Zhang, 2010). Besides that, an area of peaks range from wavelength 465cm^{-1} to 649cm^{-1} also shows the presence of Si-O-Si bending in both geopolymers (Saika & Parthasarathy, 2010) while Si-O quarts is especially obvious in GP-1M at wavelength 708.8cm^{-1} . Lastly, the wavelength area of 3400cm^{-1} which shows the H-O-H stretch due to addition of distilled water in the geopolymerization.

4.2.3. MIP Analysis

An important qualifying property for a material to be an effective adsorbent is porosity and pore volume. In order to predict the adsorption capabilities of both geopolymers synthesized, MIP has been used to determine their pore size and distribution respectively as shown in Figure 4.3 and 4.4.

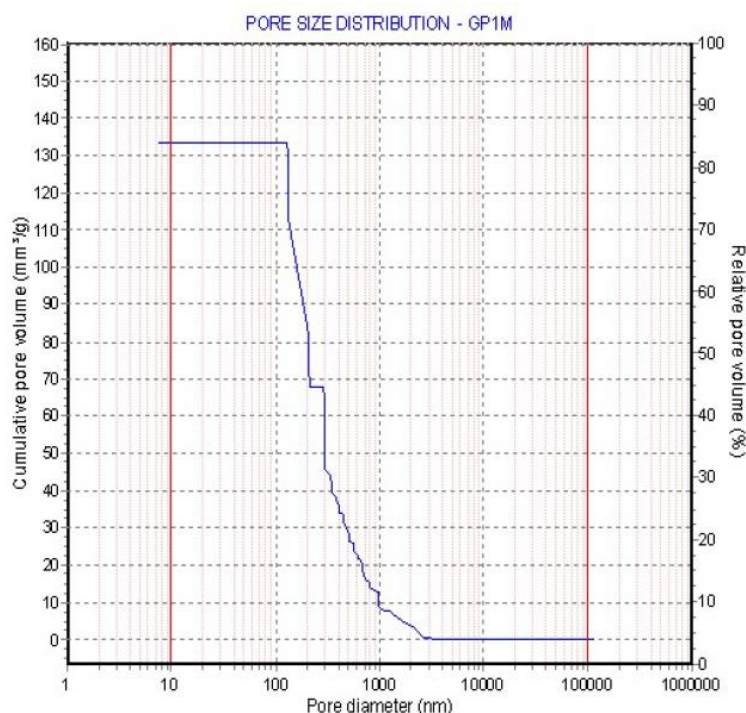


Figure 4.3- Pore size distribution of GP-1M.

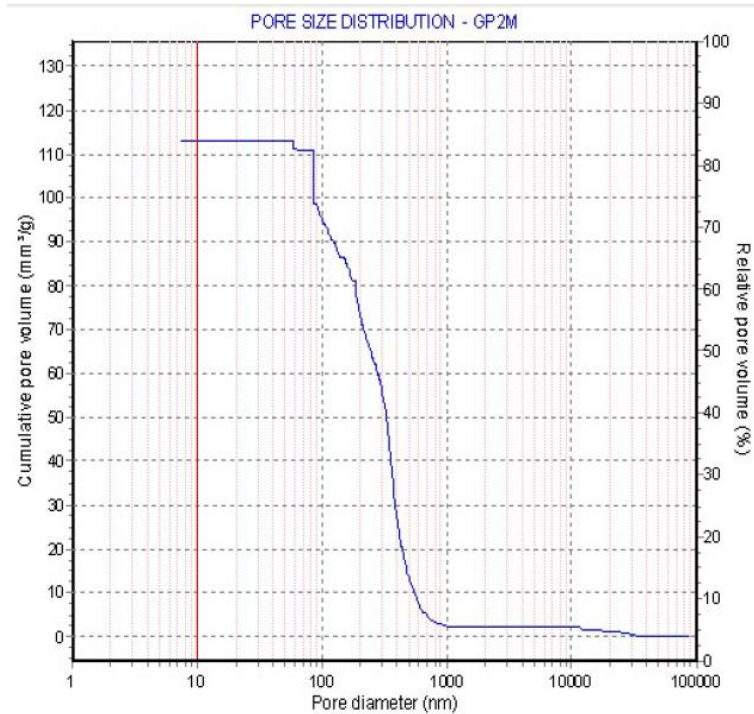


Figure 4.4- Pore size distribution of GP-2M.

As we observe from results obtained through MIP shown in Figure 4.3 and 4.4, GP-1M has a relatively higher pore volume of $133.51\text{mm}^3/\text{g}$ as compared to GP-2M which has only total pore volume of $113.09\text{mm}^3/\text{g}$. Although both geopolymers synthesized has almost similar pore surface area ($2.244\text{m}^2/\text{g}$ and $2.281\text{m}^2/\text{g}$), GP-1M has higher average pore diameter (238.02nm) as compared to GP-2M (198.33nm). Commercial zeolites is exhibiting pore volume of $242\text{mm}^3/\text{g}$ (MFI(ZSM-5), 2014) which is slightly higher than both geopolymers synthesized. Higher porosity observed in GP-1M (higher pore volume) is also expected to improve both sorption and kinetic properties of the geopolymer (Deze, Papageorgiou, Favvas, & Katsaros, 2012).

4.2.4. Particle Size Analysis (PSA)

PSA is a useful tool to determine the particle size of geopolymers. GP-1M shows a mean particle size of $4.891\mu\text{m}$ while GP-2M contains particle size of $4.207\mu\text{m}$. Finer particles size of geopolymers will provide good surface area and improve adsorption (Zainudin, Lee, Kamaruddin, Bhatia, & Mohamed, 2005). The result of PSA is presented below in Figure 4.5 and 4.6.

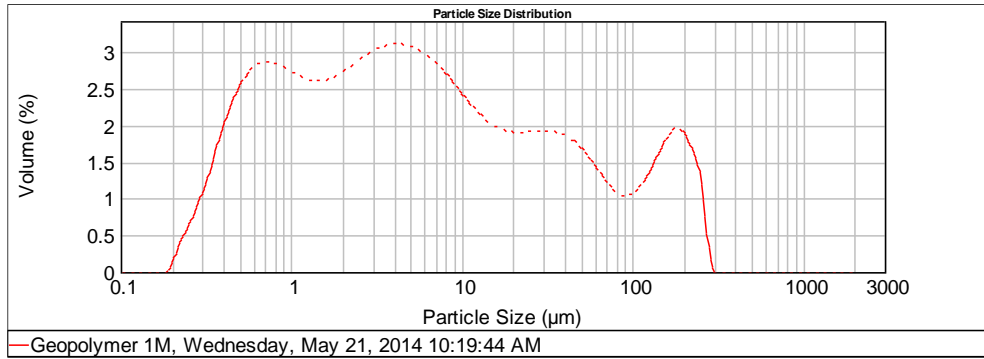


Figure 4.5- Particle size distribution curve of GP-1M.

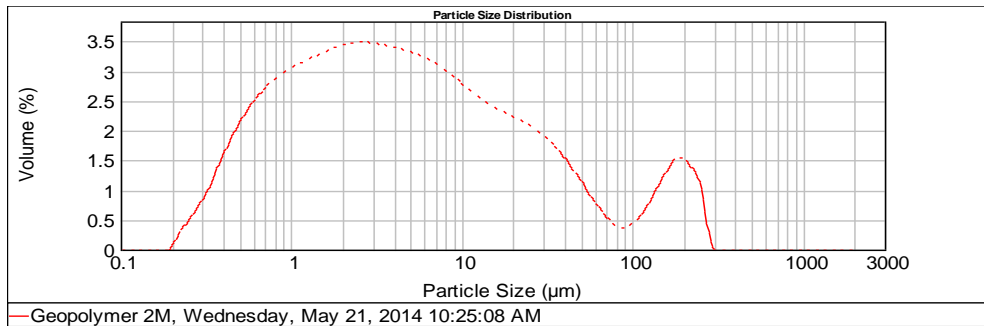


Figure 4.6- Particle size distribution curve of GP-2M.

4.2.5. FESEM Analysis

Both GP-1M and GP-2M were observed under FESEM at 1,000, 5,000 and 10,000 magnifications. The results of the analysis are shown in Figure 4.7. From image generated by FESEM shown in Figure 4.7, the porous structure can be observed obviously.

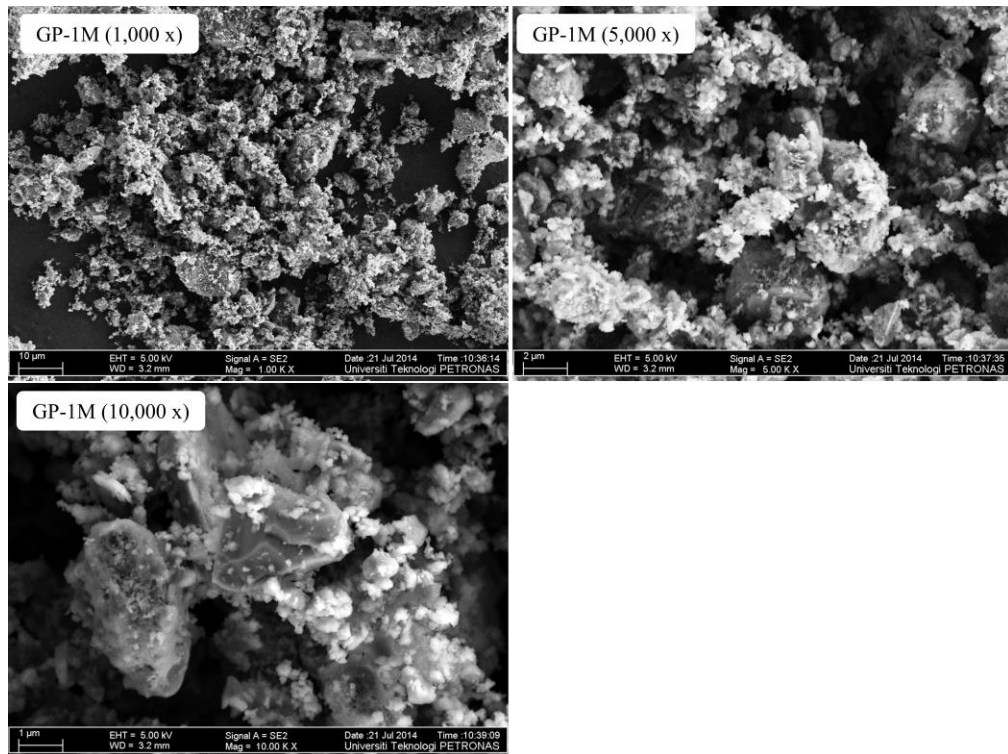


Figure 4.7- FESEM micrographs of GP-1M at 1,000, 5,000 and 10,000 magnification.

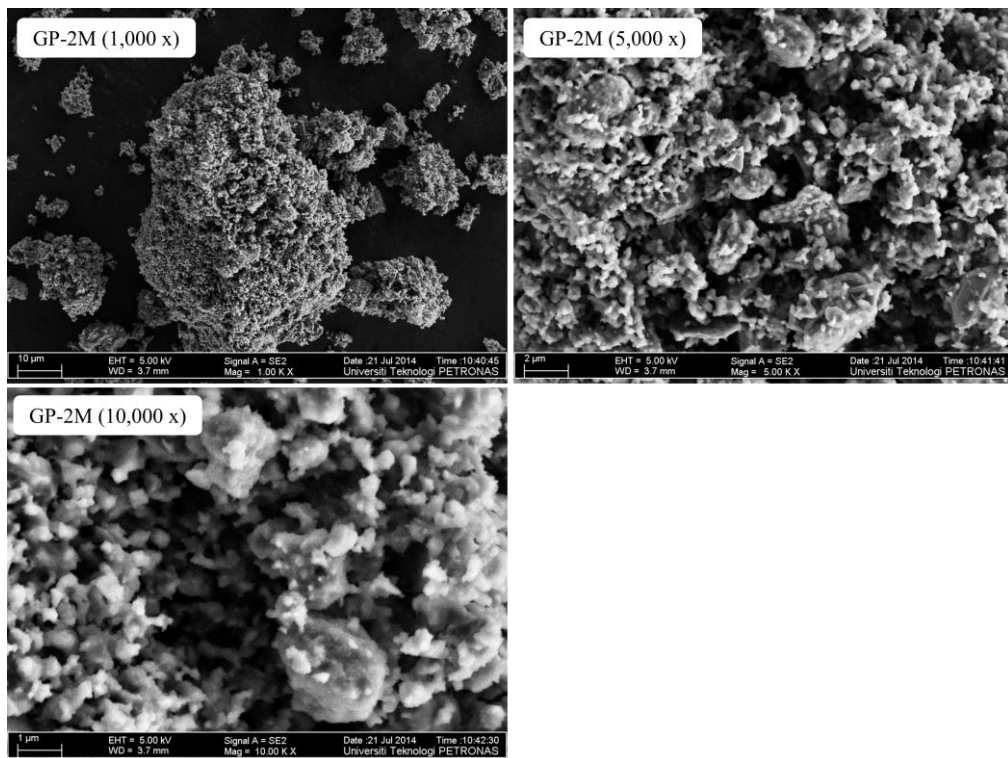


Figure 4.8- FESEM micrographs of GP-2M at 1,000, 5,000 and 10,000 magnification.

4.3. INITIAL ADSORPTION EXPERIMENT RESULT

Initial adsorption test had been carried out using methylene blue solution to determine the adsorption ability of GP-1M and GP-2M. The effect of initial adsorbent dosage and pH has been carried out to observe the adsorption process by both geopolymers.

4.3.1. Effect of initial adsorbent dosage.

The adsorption process has been carried out using 25ml of 50ppm methylene blue solution. Adsorbent dosage of 0.2g, 0.4g, 0.6g, 0.8g and 1.0g has been used to study the effect of initial dosage on adsorption capabilities of GP-1M and GP-2M. Figure 4.9 and 4.10 are the result of experiment respectively.

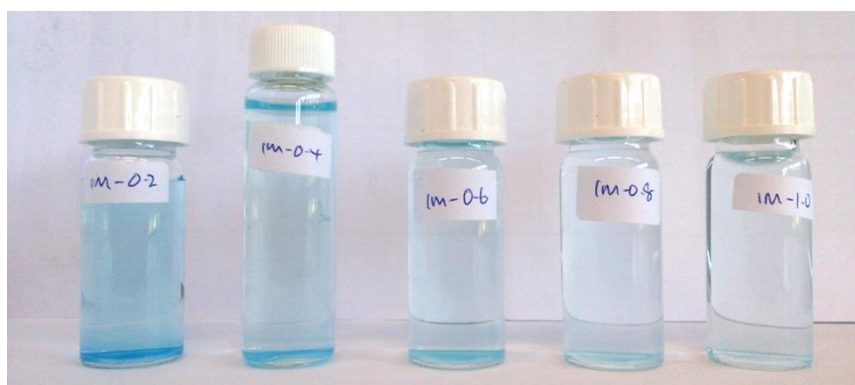


Figure 4.9- Effect of initial adsorbent dosage on methylene blue adsorption using GP-1M.

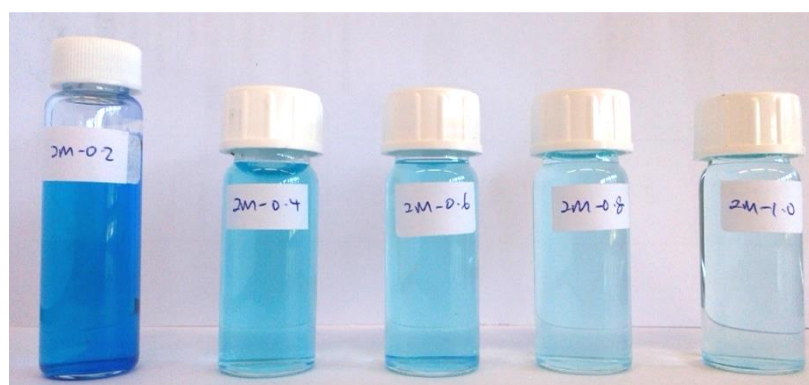


Figure 4.10- Effect of initial adsorbent dosage on methylene blue adsorption using GP-2M.

From Figure 4.9 and 4.10, the adsorption activity of methylene blue increase as the initial geopolymer dosage increase. From results shown in Figure 4.9, we observed an adsorbent dosage reach optimum at 0.4g. Besides that, the result of experiment also shows the adsorption activity of GP-1M is more active as compared to GP-2M. The final colour intensity of methylene blue solution when 0.4g GP-1M is used can only be reached using 1.0g of GP-2M. This observation is expected as the porosity of GP-1M is relatively higher than that of GP-2M.

With UV-VIS Spectrometer used, the exact concentration of methylene blue can be obtained and a graph of percent methylene blue removal versus adsorbent dosage is plotted as shown in Figure 4.11. Equation 4.1 calculates the amount total copper removal percentage.

$$\text{Percent removal, \%} = \frac{C_0 - C_1}{C_0} \times 100\% \dots\dots (4.1)$$

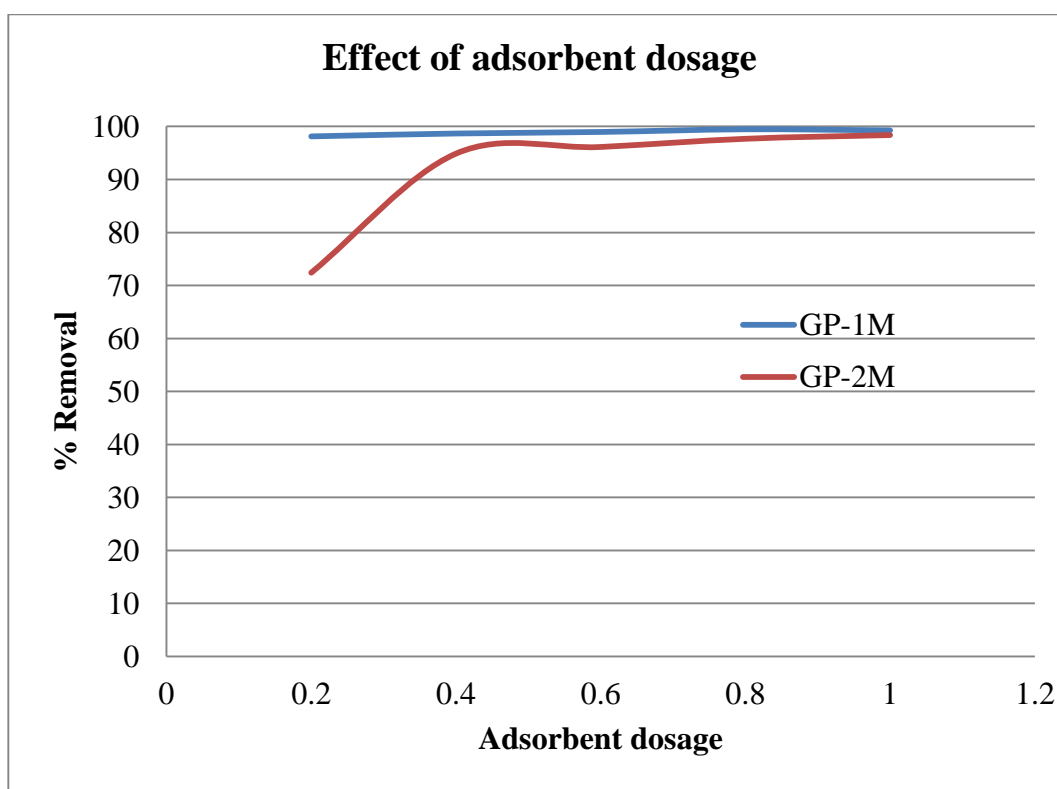


Figure 4.11- Effect of initial adsorbent dosage on methylene blue adsorption using GP-1M and GP-2M.

Figure 4.11 shows that 0.2g of GP-1M is able to achieve 98.1% removal of methylene blue while the same removal capacity was achieved only when 1g of GP-

2M was used. However, Figure 1.3 clearly shows the excellent removal capacity of methylene by both phosphoric acid-based geopolymers.

4.3.2. Effect of pH.

pH is also a significant factor in affecting the adsorption activity by geopolymers. Five different pH values (3, 5, 7, 9, and 10) have been studied and the results are as shown in Figure 4.12 and 4.13.



Figure 4.12- Effect of pH on adsorption of methylene blue using GP-1M.



Figure 4.13- Effect of pH on adsorption of methylene blue using GP-2M.

Figure 4.12 and 4.13 shows that the adsorption activities of both geopolymer increase as pH increase which is similar to previous study (Kannan & Sundaram, 2001). From the observation we can deduce that an acidic condition is unfavorable to the adsorption activities of geopolymers. Again in this experiment, we observed the difference in adsorption capabilities of GP-1M and GP-2M especially in acidic pH values.

Data obtained from analysis were used to plot graph shown in Figure 4.14, to observe the effect of pH on methylene blue solution using phosphoric acid-based geopolymers.

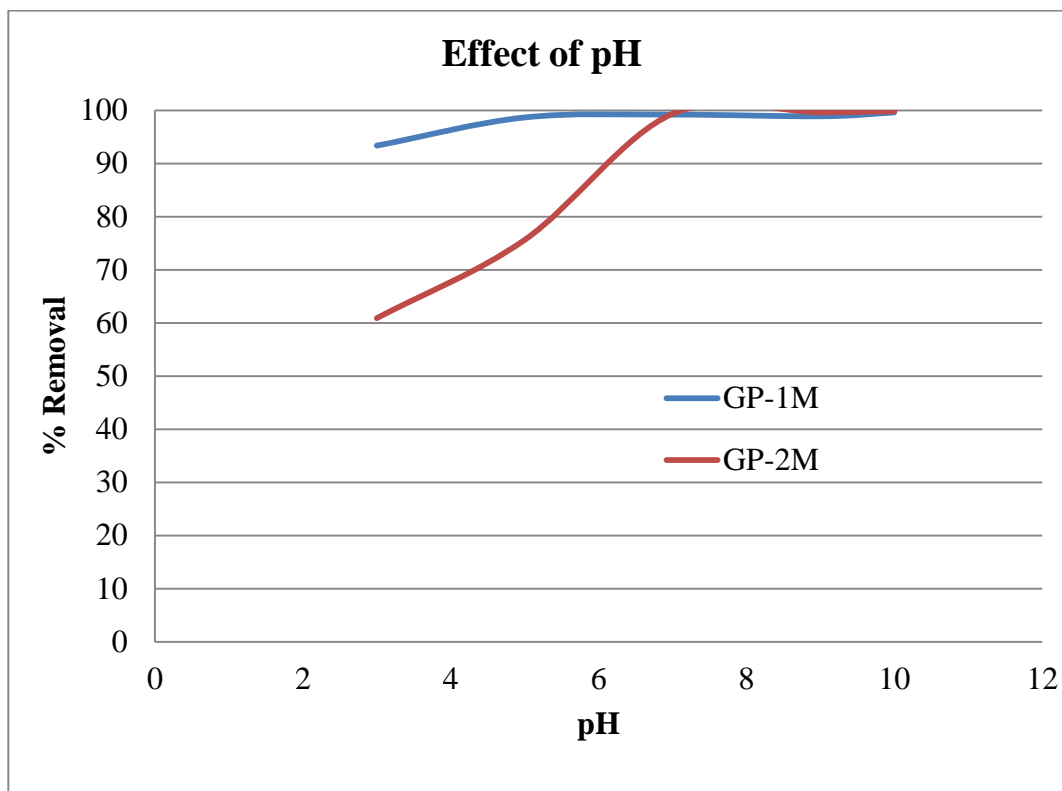


Figure 4.14- Effect of pH on the adsorption of methylene blue using GP-1M and GP-2M.

Similar to Figure 4.11, GP-1M shows better adsorption kinetics as compare to GP-2M in Figure 4.14. However, we observe an obvious increase in methylene blue removal as the pH increase. Overall methylene blue removal reaches 98-99% by both geopolymers.

4.3.3. Kinetic study

The kinetic study of GP-1M and GP-2M adsorption capabilities was observed by conducting the adsorption test under different initial methylene blue solution and sample extraction at 30 minutes interval. Experimental data was used to plot graph Figure 4.15-4.18 to study the kinetic model of adsorption activities by phosphoric acid-based geopolymers.

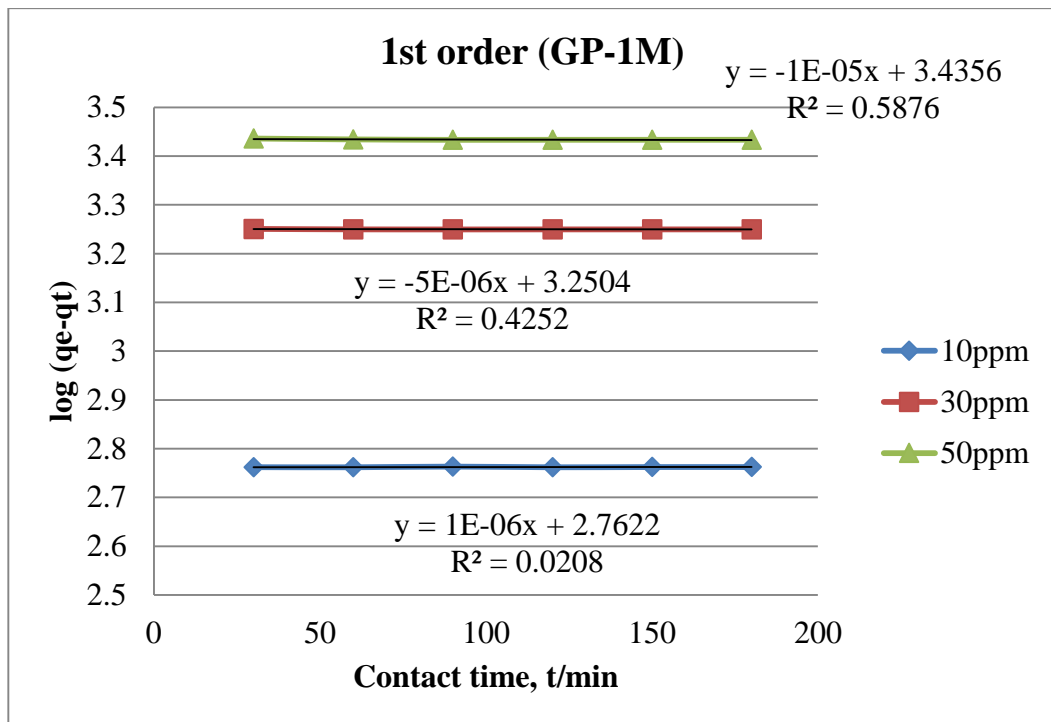


Figure 4.15- Pseudo first order kinetic model (GP-1M).

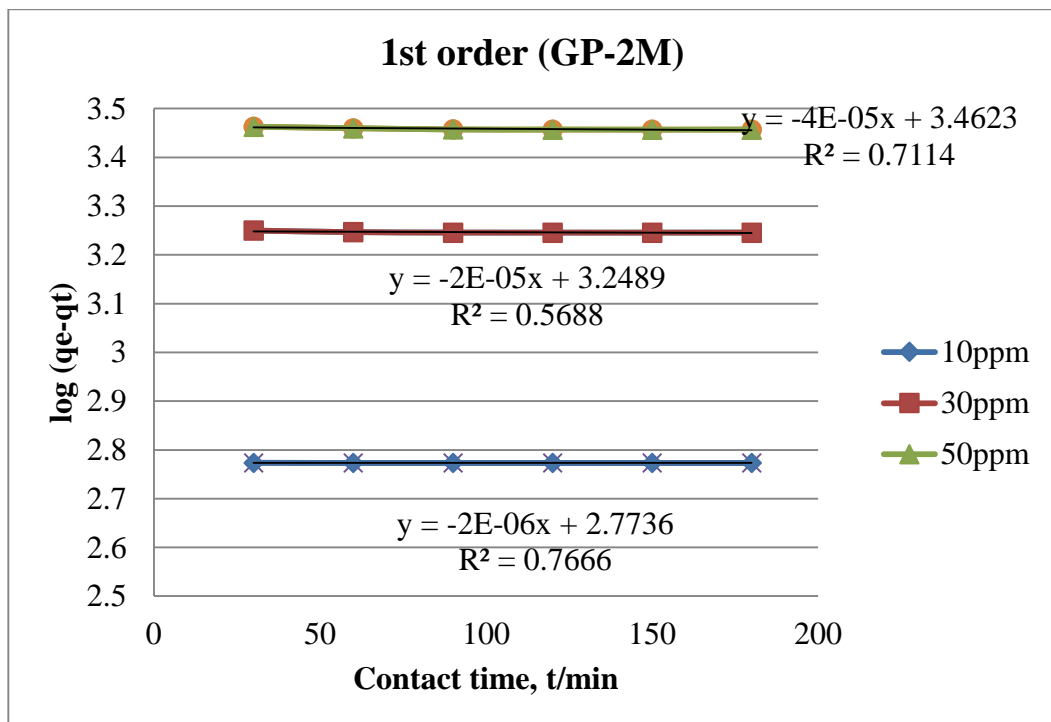


Figure 4.16- Pseudo first order kinetic model (GP-2M).

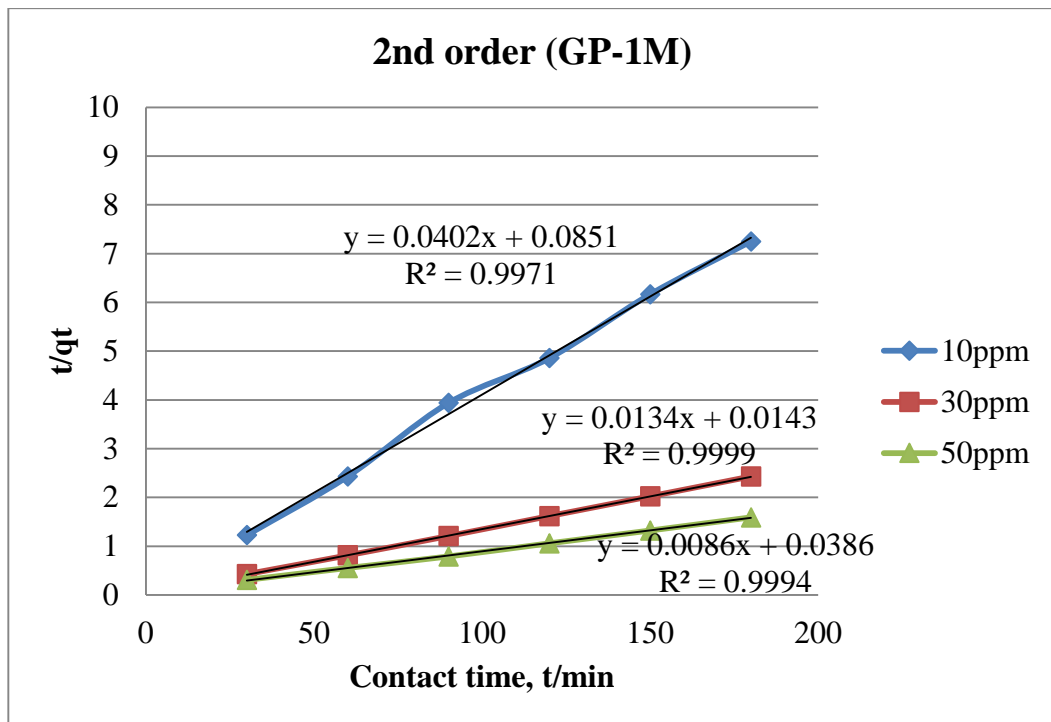


Figure 4.17- Pseudo second order kinetic model (GP-1M).

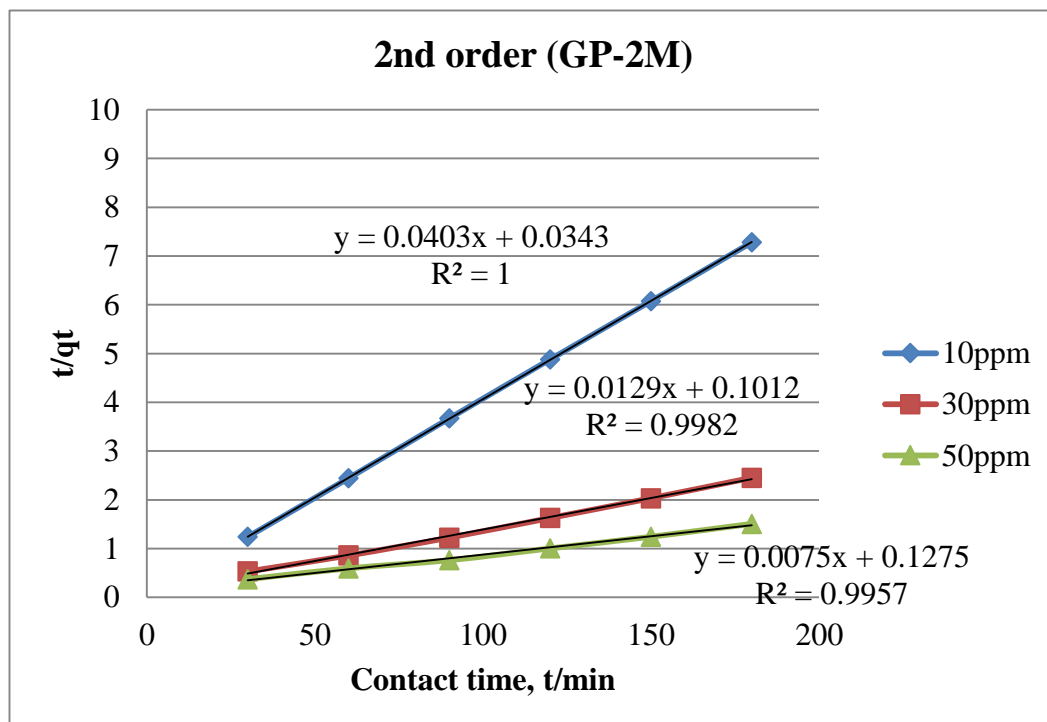


Figure 4.18- Pseudo second order kinetic model (GP-2M).

Equation 4.2 and 4.3 shows respectively the equation for both pseudo first order and second order reaction.

$$\log(q_e - q_t) = \log q_e - \left(\frac{k_1}{2.303}\right)t \dots\dots (4.2)$$

$$\frac{t}{q_t} = \frac{1}{k_2 q_e^2} + \left(\frac{1}{q_e}\right)t \dots\dots (4.3)$$

Where q_t is the amount adsorbed (mg/g) at time t and the amount adsorbed at equilibrium, q_e can be determined using Equation 4.4.

$$q_e = \frac{(c_i - c_e)V}{M}$$

Where

- $k_1 =$ Rate constant for pseudo first order rate of reaction model
- $k_2 =$ Rate constant for pseudo second order rate of reaction model
- $c_i =$ Initial adsorbate concentration
- $c_e =$ Adsorbate concentration at equilibrium
- $V =$ Volume of solution, ml
- $M =$ Mass of adsorbent used, g

Table 4.3 shows the comparison of k_1 , q_e and R^2 values obtained from Figure 4.15 to 4.16.

TABLE 4.3- Comparison of k_1 , q_e and R^2 values of GP-1M and GP-2M for pseudo first order reaction model for methylene blue adsorption.

Type of geopolymers	Initial solution concentration, ppm	k_1 (g/mg.min)	R^2	q_e from graph (mg/g)
GP-1M	10	-6.3609	0.02	578.0960
	30	-7.4848	0.425	1778.2794
	50	-7.9108	0.587	2722.7013
GP-2M	10	-6.3862	0.766	592.9253
	30	-7.4801	0.568	1770.1090
	50	-7.9730	0.711	2897.3436

Table 4.4 shows the comparison result of k_2 , q_e and R^2 values for pseudo second order reaction model of GP-1M and GP-2M as shown in Figure 4.17 and 4.18.

TABLE 4.4- Comparison of k_2 , q_e and R^2 values of GP-1M and GP-2M for pseudo second order reaction model for methylene blue adsorption.

Type of geopolymers	Initial solution concentration, ppm	k_2 (g/mg.min)	R^2	q_e from graph (mg/g)
GP-1M	10	0.0188	0.997	25.0000
	30	0.0121	0.999	76.9231
	50	0.0017	0.999	125.0000
GP-2M	10	0.0471	1.000	25.0000
	30	0.0014	0.998	83.3333
	50	0.0004	0.995	142.8571

Results show that the adsorption activities of both GP-1M and GP-2M fitted well into pseudo second order kinetic model at various initial concentration.

4.3.4. Isotherm Study

Isotherm study was conducted using the same experiment data obtained from kinetic study experiment. Figure 4.19-4.22 shows the Langmuir and Freundlich isotherms plotted for both GP-1M and GP-2M.

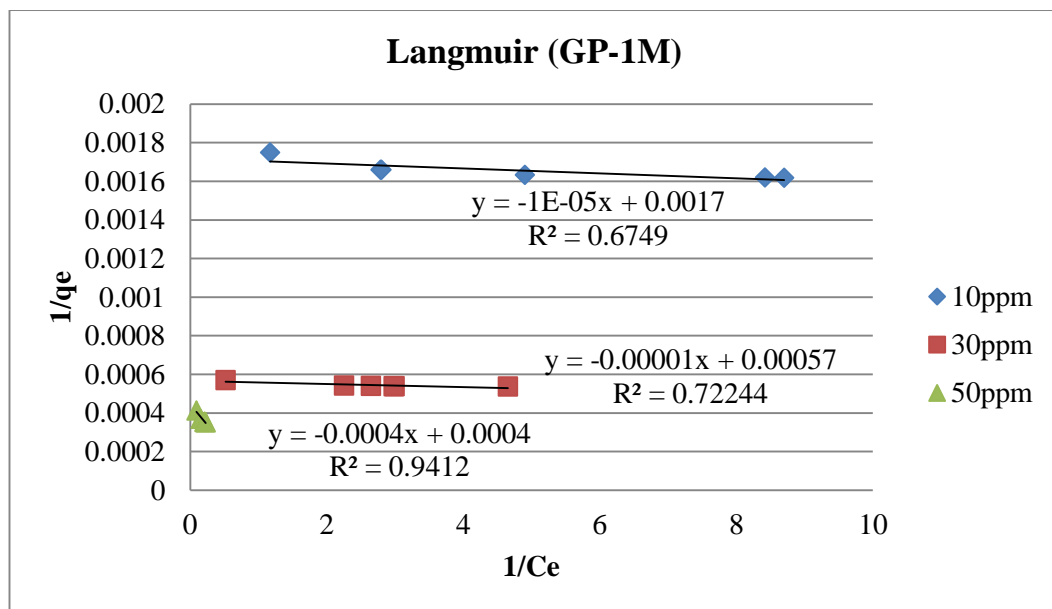


Figure 4.19- Langmuir isotherm (GP-1M).

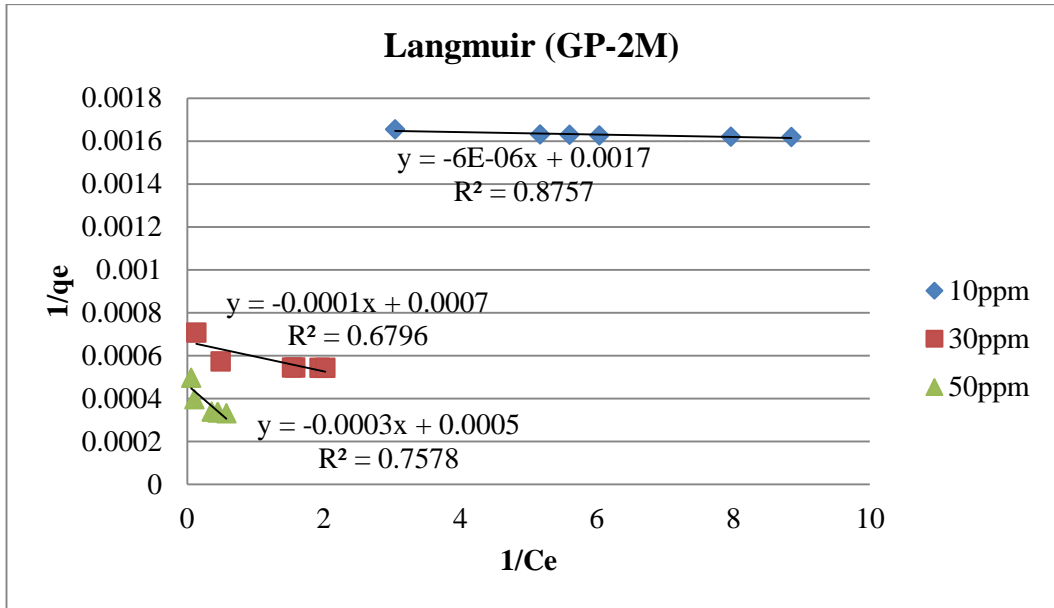


Figure 4.20- Langmuir isotherm (GP-2M).

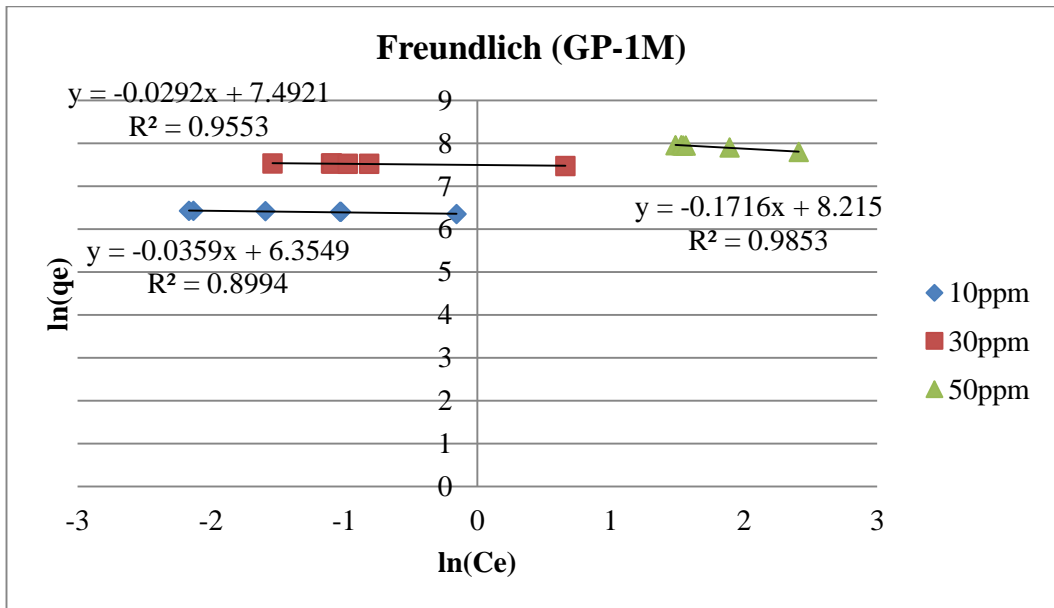


Figure 4.21- Freundlich isotherm (GP-1M).

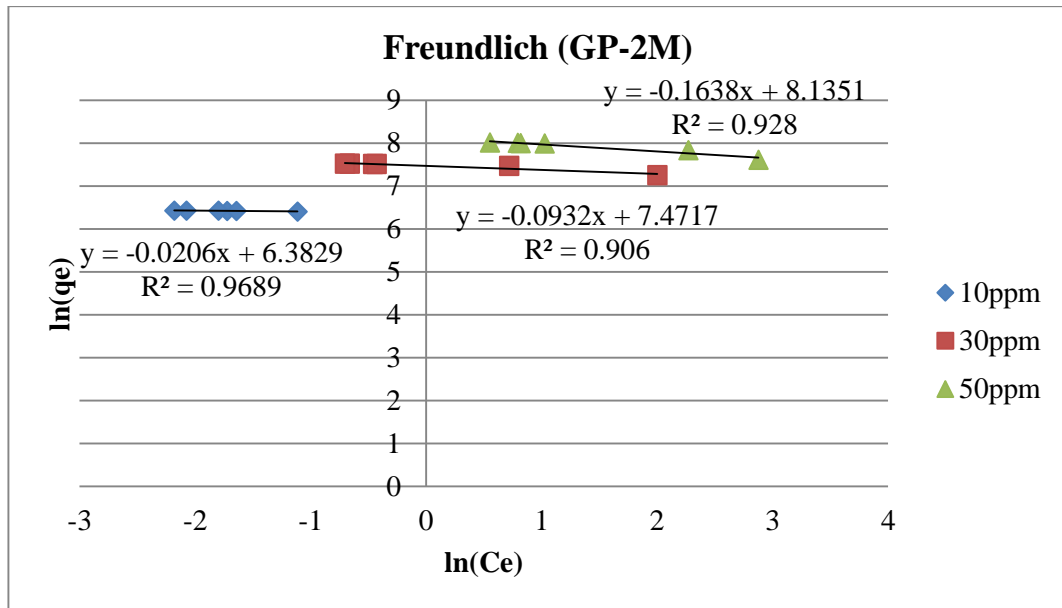


Figure 4.22- Freundlich isotherm (GP-2M).

Equation 4.4 shows the relationship between q_e and C_e for Langmuir Isotherm.

$$\frac{1}{q_e} = \frac{1}{q_m K_L} \left(\frac{1}{C_e} \right) + \frac{1}{q_m} \dots\dots (4.4)$$

Where

q_m = Maximum amount of adsorbates adsorbed into the adsorbent, mg/g

K_L = Langmuir constant of adsorption, L/mg

(Cheng, Lee, Ko, Ueng, & Yang, 2012)

For Freundlich isotherm, the relationship between q_e and C_e can be represented using correlations as shown in Equation 4.5 below.

$$\ln q_e = \ln K_F + \frac{1}{n} \ln C_e \dots\dots (4.5)$$

Where

K_F = Indicators of adsorption capacity

n = Adsorption intensity

(Hameed, 2008)

Summary on the values of unknowns and constants in Equation 4.4 and 4.5 is tabulated in Table 4.5 and 4.6 after calculations.

TABLE 4.5- Values of Langmuir isotherm constants for GP-1M and GP-2M in methylene blue adsorption test.

Type of geopolymers	Initial solution concentration, ppm	q_m	K_L	R^2
GP-1M	10	1000.0000	-100.0000	0.674
	30	1754.3860	-57.0000	0.72244
	50	2500.0000	-1.0000	0.9412
GP-2M	10	1000.0000	-166.6667	0.875
	30	1428.5714	-7.0000	0.6796
	50	2000.0000	-1.6667	0.7578

TABLE 4.6- Values of Freundlich isotherm constants for GP-1M and GP-2M in methylene blue adsorption test.

Type of geopolymers	Initial solution concentration, ppm	n	K_F	R^2
GP-1M	10	-28.5714	574.7873	0.899
	30	-34.4828	1793.6358	0.955
	50	-5.8480	3695.9762	0.985
GP-2M	10	-50.0000	591.1087	0.968
	30	-10.7527	1756.3622	0.906
	50	-6.1350	3411.8161	0.928

Results obtained shows that adsorption activities of GP-1M and GP-2M fitted well into Freundlich isotherm as compared to Langmuir isotherms due to high correlation factor, R^2 were observed.

4.4. ADSORPTION TEST RESULT

Adsorption of Copper (II) ions has been carried out using copper nitrate solution ($\text{Cu}(\text{NO}_3)_2$). GP-1M and GP-2M has been used as adsorbents to remove copper ions in the solution.

4.4.1. Effect of pH

Adsorption activity is highly affected by pH and in this research, pH of 3,5 7, 9 and 10 has been studied and the result is shown in Figure 4.23.

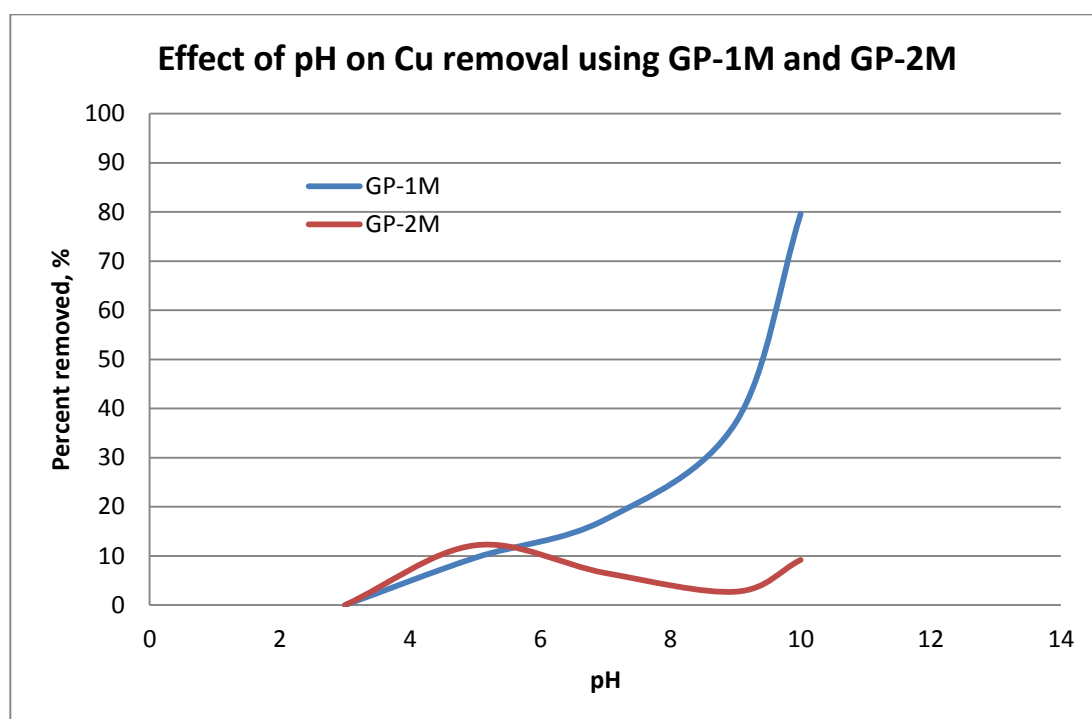


Figure 4.23- Effect of pH on Cu^{2+} adsorption.

Figure 4.23 shows that the adsorption activities take place and increase with pH. Besides that, distinction between adsorption capabilities of geopolymers can be observed clearly in the figure. GP-1M shows a gradual increasing trend of adsorption curve while GP-2M shows unstable and poor adsorption of copper ions. A sudden increase in copper removal by GP-1M observed at pH 8 which is actually due to the precipitation of copper hydroxide ($\text{Cu}(\text{OH})_2$) when sodium hydroxide (NaOH) is added initially to increase initial solution pH (Aydin, Bulut, & Yerlikaya, 2008) (Tumin, Chuah, Zawani, & Abdul Rashid, 2008). The low percent removal of copper ions at acidic pH is due to the present of H_3O^+ which eventually competes with Cu^{2+}

for adsorption site (Tumin, Chuah, Zawani, & Abdul Rashid, 2008) (Aydin, Bulut, & Yerlikaya, 2008).

4.4.2. Effect of Contact time

The effect of contact time on the adsorption activities of geopolymers can be summarized in Figure 4.24 below.

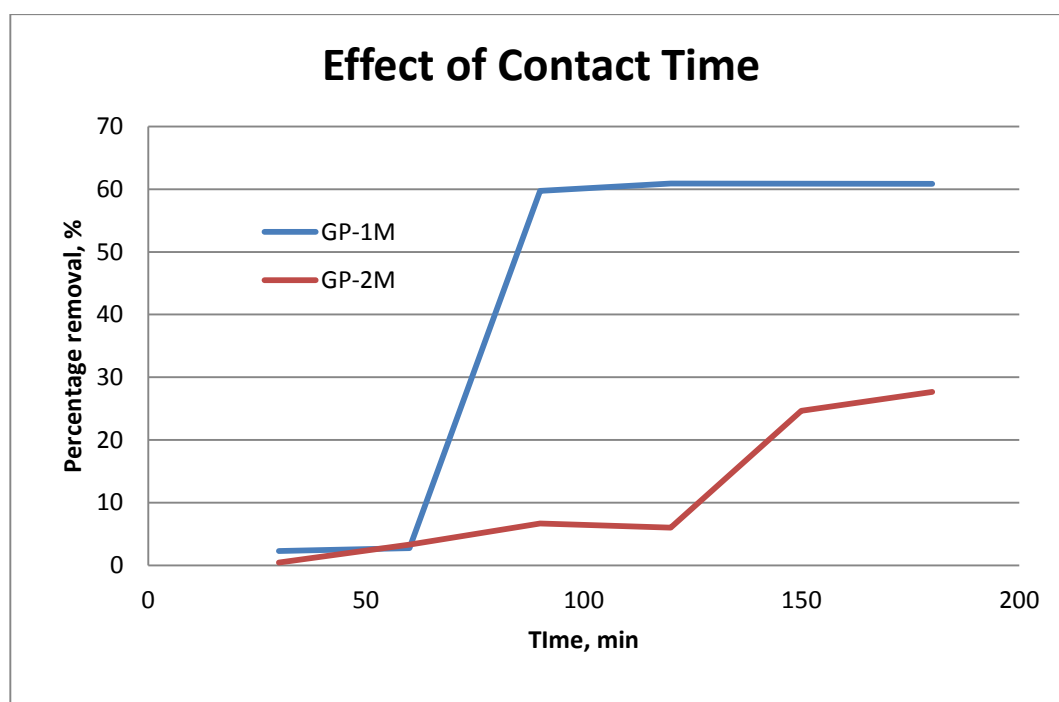


Figure 4.24- Effect of contact time.

Figure 4.24 has clearly shows the equilibrium curve of adsorption by GP-1M and GP-2M. A 60% copper ions removal was achieved by GP-1M while only around 28% removal was achieved by GP-2M. Besides that, it is observed that GP-1M reaches equilibrium faster (at 90 min) then GP-2M (at 180min). The results obtained from experiment will also be used for kinetic and isotherms studies.

4.4.3. Kinetic study of Adsorption

Pseudo first order and second order equations are applied to determine the kinetic of adsorption activity for both GP-1M and GP-2M.

Graphs of $\log(q_e - q_t)$ vs t has been plotted to demonstrate the adsorption activities of GP-1M and GP-2M correspond to pseudo first order reaction as shown in Figure 4.25 and 4.26.

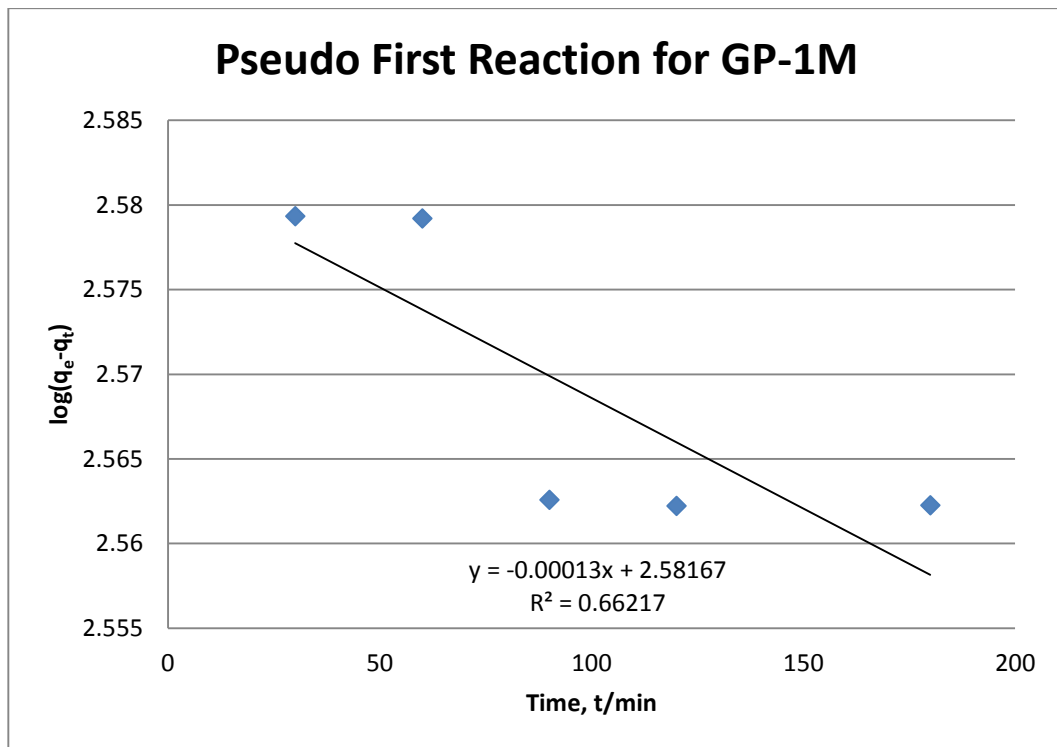


Figure 4.25- Pseudo first reaction model for GP-1M.

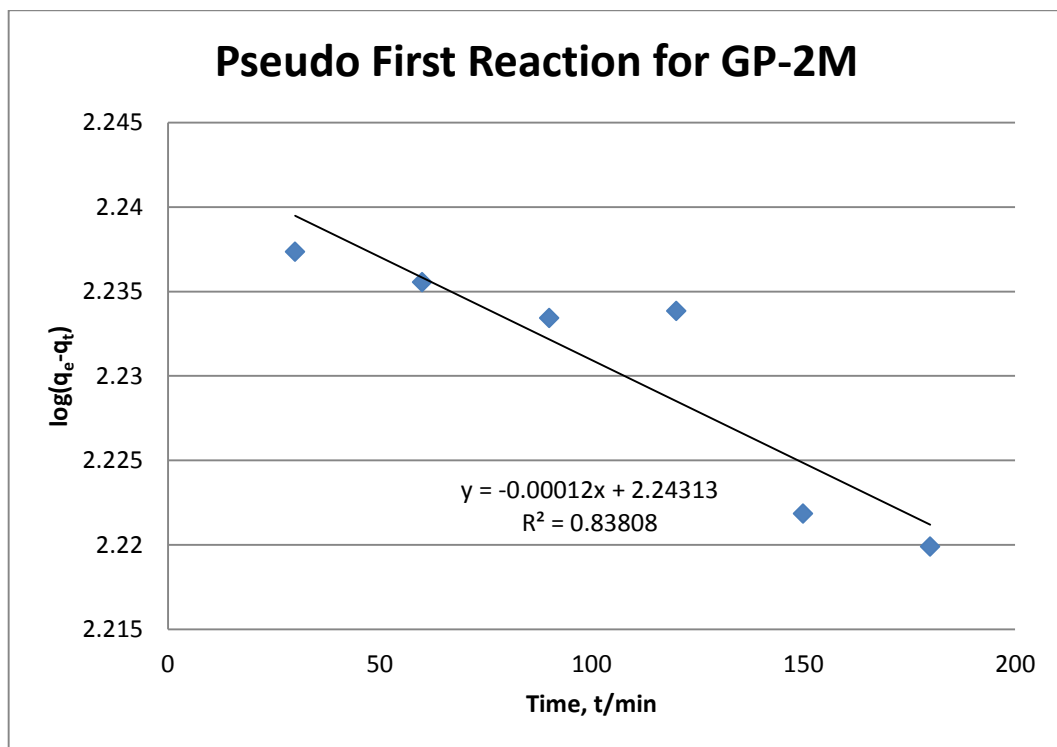


Figure 4.26- Pseudo first reaction model for GP-2M.

From Figure 4.25 and Equation 4.2, the value of k_1 for GP-1M is determined through the gradient of the graph.

$$\frac{k_1}{2.303} = 0.00013$$

$$k_1 = 2.9939 \times 10^{-4} \text{ g/mg} \cdot \text{min}$$

Using the Equation 4.2, the pseudo first order reaction rate constant for GP-2M was obtained as $2.7636 \times 10^{-4} \text{ g/mg} \cdot \text{min}$. Table 4.7 shows the comparison of k_1 , q_e and R^2 values obtained from Figure 4.25 and 4.26.

TABLE 4.7- Comparison of k_1 , q_e and R^2 values of GP-1M and GP-2M for pseudo first order reaction model.

Type of geopolymers	k_1 (g/mg.min)	q_e (mg/g)	R^2	q_e from graph (mg/g)
GP-1M	2.9939×10^{-4}	380.175	0.66217	381.654
GP-2M	2.7636×10^{-4}	172.8375	0.83808	175.037

For pseudo second order reaction model, graphs of t/q_t vs t have been plotted as shown in Figure 4.27 and 4.28.

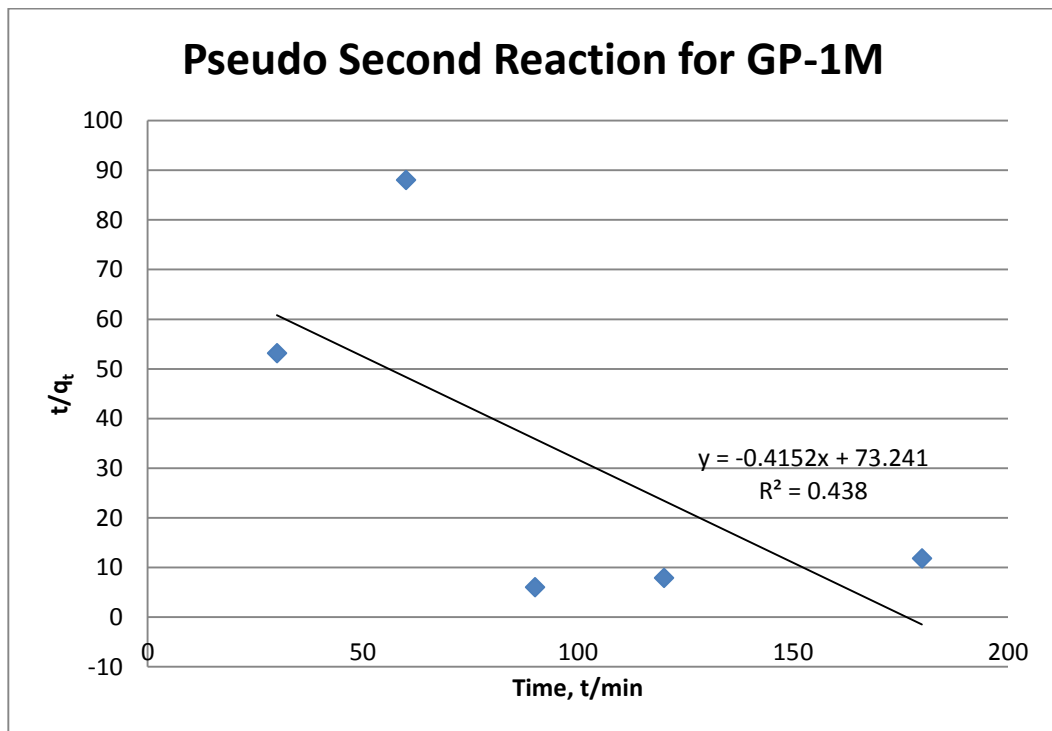


Figure 4.27- Pseudo second reaction model for GP-1M.

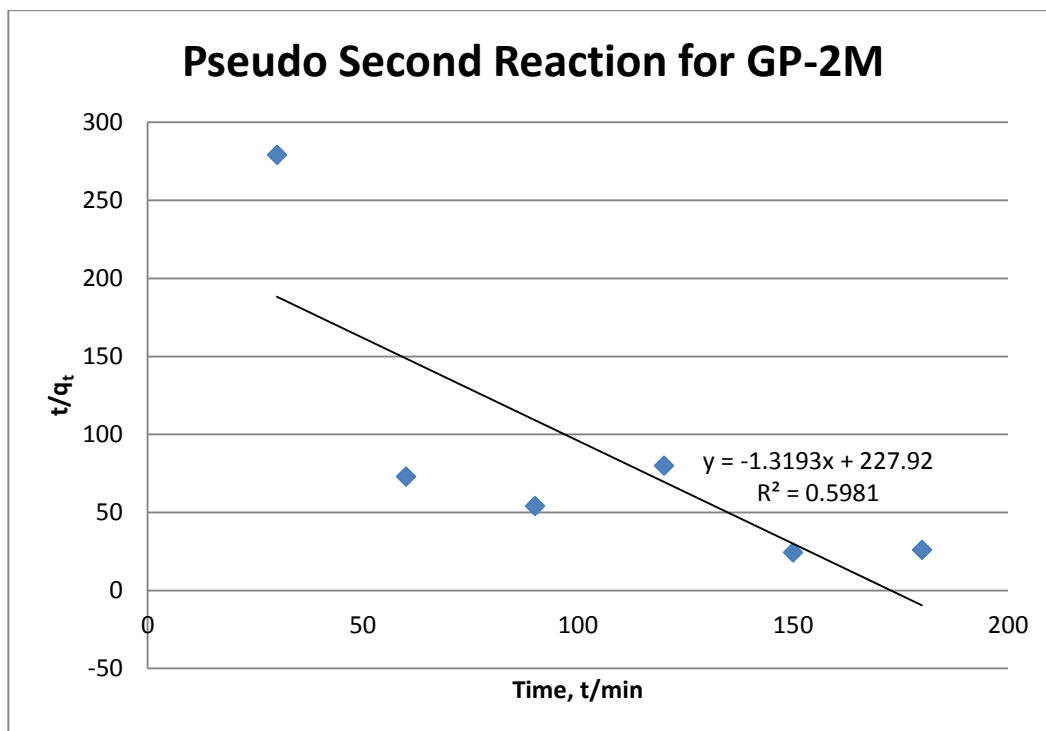


Figure 4.28- Pseudo second reaction model for GP-2M.

Using Equation 4.3 as guide, the gradient of Figure 4.27 and 4.28 is equal to $1/q_e$ and the y-intercept of the graphs is represent by $1/(k_2q_e)^2$. Table 4.7 shows the comparison result of k_2 , q_e and R^2 values for pseudo second order reaction model of GP-1M and GP-2M.

TABLE 4.8- Comparison of k_2 , q_e and R^2 values of GP-1M and GP-2M for pseudo second order reaction model.

Type of geopolymers	k_2 (g/mg.min)	q_e from graph (mg/g)	R^2
GP-1M	2.3516×10^{-3}	-2.4096	0.438
GP-2M	2.3751×10^{-2}	-0.7582	0.598

As we compare the R^2 values tabulated in Table 4.7 and 4.8, we can deduce that the adsorption activities of both geopolymers fitted pseudo first order reaction kinetic model. The q_e values calculated from the graph equation show high agreement with the experimental values and the value of R^2 is also relatively higher as compare to using pseudo second order reaction kinetic model. These had indicates

that the pseudo first order reaction kinetic model best describe the adsorption activities of GP-1M and GP-2M.

4.4.4. Isotherms studies of Adsorption

Langmuir and Freundlich Isotherms have been plotted to investigate which isotherms best fitted the adsorption activities of phosphoric acid-based geopolymers. Figure 4.29 and 4.30 shows the Langmuir Isotherm plotted on experimental data obtained from adsorption process using GP-1M and GP-2M respectively.

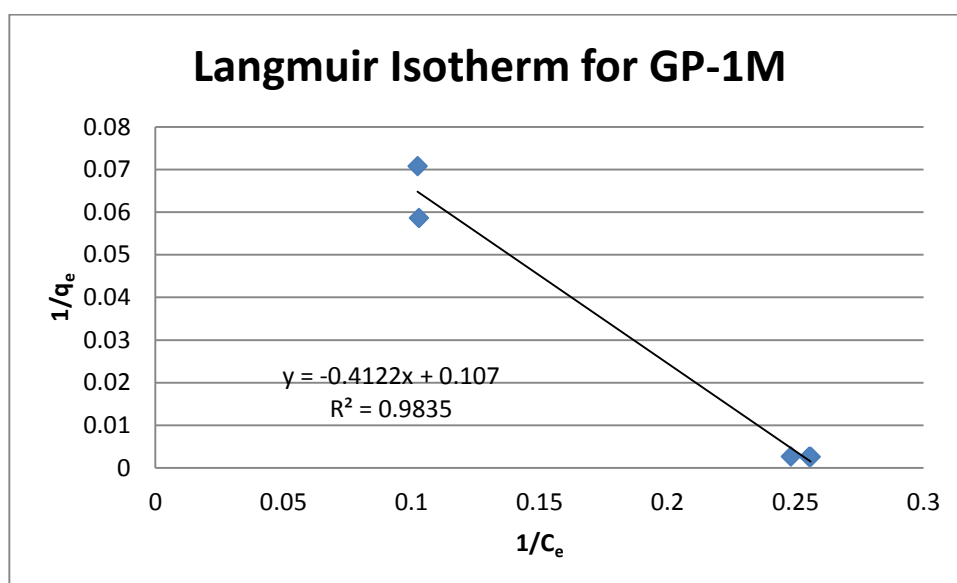


Figure 4.29- Langmuir Isotherm for GP-1M.

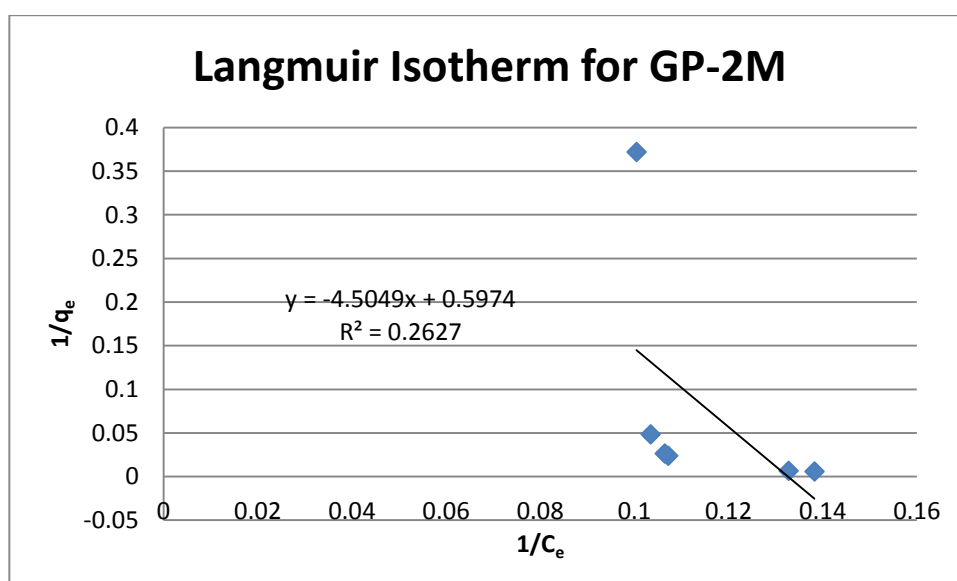


Figure 4.30- Langmuir Isotherm for GP-2M.

Figure 4.31 and 4.32 shows the Freundlich isotherms of GP-1M and GP-2M.

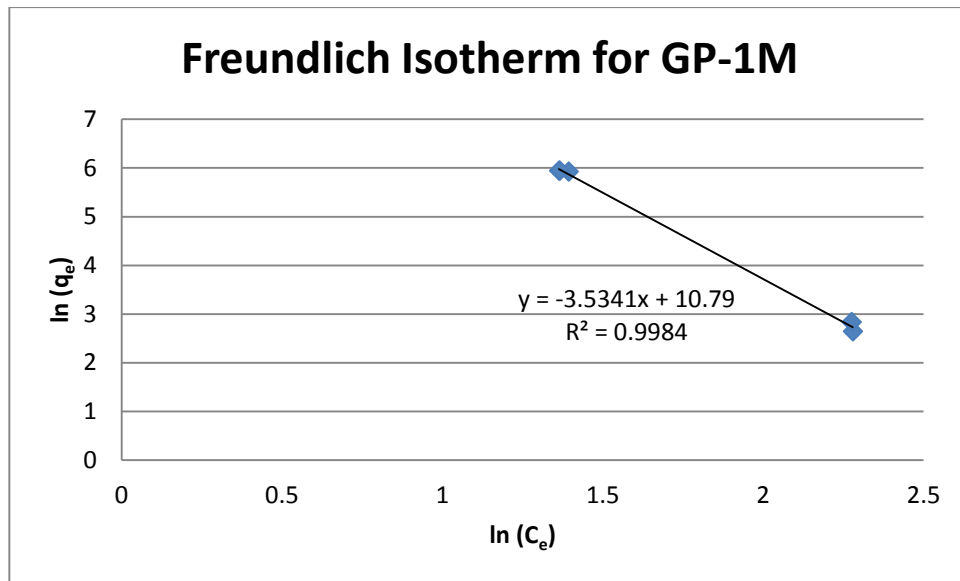


Figure 4.31- Freundlich Isotherm for GP-1M.

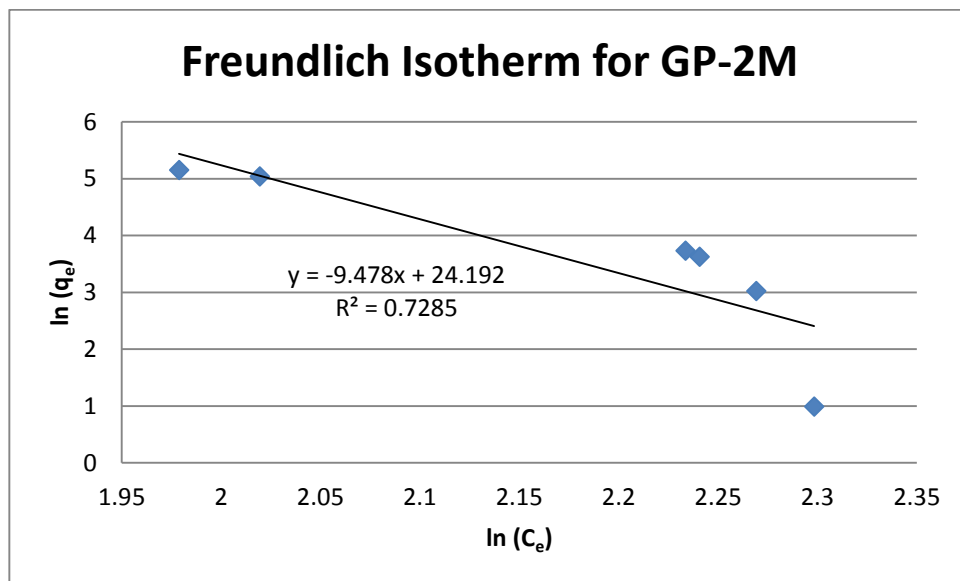


Figure 4.32- Freundlich Isotherm for GP-2M.

The best fitted isotherm for the adsorption activities will be determined using the highest R^2 values obtained from the isotherm graph. Hence, the adsorption activities of GP-1M and GP-2M fitted Freundlich Isotherms due to higher R^2 values obtained from isotherms plotted as compared to Langmuir Isotherm.

Summary on the values of unknowns and constants in Equation 4.4 and 4.5 is tabulated in Table 4.9 after calculations.

TABLE 4.9- Values of Langmuir and Freundlich constants for GP-1M and GP-2M.

Type of Geopolymers	Langmuir Isotherm			Freundlich Isotherm		
	q_m	K_L	R^2	K_F	n	R^2
GP-1M	9.3458	-0.2597	0.983	48,533.04	-0.2830	0.998
GP-2M	1.6750	-0.1326	0.262	3.203×10^{10}	-0.1055	0.728

CHAPTER FIVE

CONCLUSION & RECOMMENDATIONS

5.1. CONCLUSION

The phosphoric acid-based geopolymers with high porosity has been successfully synthesized by mixing method. From the two geopolymers produced, GP-1M with 1:1 alumina to phosphate ratio exhibit a better adsorbent properties as compared to GP-2M which has 1:1.2 alumina to phosphate ratio.

Results from MIP has shown the overall porosity of GP-1M is higher than that of GP-2M, thus concluded the adsorption capacity of GP-1M is as well higher than that of GP-2M. FTIR studies also deduced the formation of berlinite and crystalline quartz, confirming the existent of geopolymerization. FESEM results show the porous surface structure of geopolymers, confirming the adsorbents quality in the synthesized phosphoric acid-based geopolymers.

In the adsorption test, the adsorption activities of geopolymers are hindered at both extreme acidic or alkaline conditions. The optimum pH for phosphoric acid-based geopolymers is 6.5. The adsorption kinetic of both geopolymers fitted the pseudo second order reaction kinetic model. GP-1M's and GP-2M's adsorption activities also fitted the Freundlich Isotherm.

This project has successfully proven the adsorption capabilities of phosphoric acid-based geopolymers and it was clearly proven that the alumina to phosphate ratio of 1:1 produces a better adsorbent type of phosphoric acid-based geopolymers.

5.2. RECOMMENDATIONS

For future works, it is suggested that more properties of phosphoric acid-based geopolymers can be tested and identify. For instance, the effect of solution pH on the compressive strength of geopolymers and the thermal stability of geopolymers can be studied. Phosphoric acid-based geopolymers are new type of adsorbent

materials which have high potential in replacing current adsorbent in used; deeper studies of these materials would improve its adsorption capabilities.

As this project only study upon the removal of copper (II) ions, it is recommended that more heavy metal ions should be placed into test. Industrial samples could also be obtained to study how the adsorption activities by varying the concentration of various heavy metals.

Desorption test should be study to investigate the practicality and lifespan of geopolymers.

REFERENCES

- Abell, A. B., Willis, K. L., & Lange, D. A. (1999). Mercury Intrusion Porosimetry and Image Analysis of Cement-based Materials. *Journal of Colloid and Interface Science* , 39-44.
- Adsorption technologies*. (2011). Retrieved February 22, 2014, from CO2CRC: http://www.co2crc.com.au/research/demo_precomb_adsorption.html
- Allahverdi, A., Mehrpour, K., & Kani, E. N. (2008). Taftan Pozzolan-based Geopolymer Cement. *IUST Internation Journal of Engineering Science, Vol 19, No 3* , 1-5.
- Al-Zboon, K., Al-Harashseh, M. S., & Hani, F. B. (2011). Fly ash-based geopolymer for Pb removal from aqueous solution. *Journal of Hazardous Materials 188 (2011) Science Direct* , 414-421.
- Bagheri, H., Afkhami, A., Saber-Tehrani, M., & Khoshsafar, H. (2012). Preparation and characterization of magnetic nanocomposite of Schiff base/silica/magnetite as a preconcentration phase for the trace determination of heavy metal ions in water, food and biological samples using atomic absorption spectrometry. *Talanta, Vol 97* , 87-95.
- Bakharev, T. (2005). Durability of geopolymer materials in sodium and magnesium sulfate solution. *Cement and Concrete Research 35* , 1233-1246.
- Bakharev, T. (2005). Geopolymeric materials prepared using Class F fly ash and elevated temperature curing. *Cement and Concrete Research 35* , 1224-1232.
- Barakat, M. (2010). New Trends in Removing Heavy Metals From Industrial Wastewater. *Arabian Journal of Chemistry (2011) 4* , 361-377.
- Brunauer-Emmett-Teller (BET) Surface Area Analysis and Barrett-Joyner-Halenda (BJH) Pore Size and Volume Analysis*. (n.d.). Retrieved April 3rd, 2014, from Lucideon: <http://www.ceram.com/testing-analysis/techniques/brunauer-emmett-teller-surface-area-analysis-barrett-joyner-halenda-pore-size-and-volume-analysis/>
- Cheng, T. W., Lee, M. L., Ko, M. S., Ueng, T. H., & Yang, S. F. (2012). The heavy metal adsorption characteristics on metakaolin-based geopolymer. *Applied Clay Science 56 (2012), Science Direct* , 90-96.
- Copper Poisoning*. (2012, September 12). Retrieved May 13, 2014, from Medline Plus: <http://www.nlm.nih.gov/medlineplus/ency/article/002496.htm>
- Crini, G., & Badot, P.-M. (2008). Application of chitosan, a natural aminopolysaccharide, for dye removal from aqueous solutions by adsorption

processes using batch studies: A review of recent literature. *Progress in Polymer Science*, Vol 33, Issue 4 , 399-447.

Davidovits, J. (2013, January). Geopolymer Cement. *Institut Géopolymère* . Saint-Quentin, France: Institut Géopolymère.

Davidovits, J. (2011). *Geopolymer Chemistry and Applications*, 3rd ed. Saint-Quentin, France: Institut Géopolymère.

Dent, G. (n.d.). *Preparation of Samples for IR Spectroscopy as KBr Disks*. Retrieved May 25, 2014, from The Internet Journal of Vibrational Spectroscopy: <http://www.ijvs.com/volume1/edition1/section1.html>

DeSousa, T., & Webb, P. A. (2010, June 1). *SPECIAL SECTION/INSTRUMENTATION: Mercury Intrusion Porosimetry*. Retrieved May 22, 2014, from Ceramic Industry: <http://www.ceramicindustry.com/articles/special-section-instrumentation-mercury-intrusion-porosimetry>

Discharged and treatment of municipal waste water, 2012. (2012). Retrieved April 01, 2014, from Statistics Norway: <http://www.ssb.no/en/natur-og-miljo/statistikker/avlut>

Dissolved Metals Removal from Wastewater. (2014). Retrieved May 13, 2014, from evoqua water technologies: http://www.water.siemens.com/en/applications/wastewater_treatment/metals-removal/Pages/default.aspx

Douiri, H., Louati, S., Baklouti, S., Arous, M., & Fakhfakh, Z. (2014). Structural, thermal and dielectric properties of phosphoric acid-based geopolymers with different amounts of H₃PO₄. *Material Letters* 116 , 9-12.

Fourier Transform Infrared Spectroscopy. (2014, May 8). Retrieved May 26, 2014, from Wikipedia: http://en.wikipedia.org/wiki/Fourier_transform_infrared_spectroscopy

Gallé, C. (2001). Effect of drying on cement-based materials pore structure as identified by mercury intrusion porosimetry. A comparative study between oven-, vacuum-, and freeze-drying. *Cement and Concrete Research* 31 , 1467-1477.

Geankoplis, C. J. (2003). *Transport Processes and Separation Process Principles (includes unit operations)* 4th ed. New Jersey: Pearson Education International.

Geopolymer Research. (n.d.). Retrieved May 26, 2014, from UNSW Australia Canberra: http://seit.unsw.adfa.edu.au/research/details2.php?page_id=796

Ho, K. M. (2012). *Geopolymer-based Coating Material for Metal Substrate*. Tronoh: Universiti Teknologi Petronas.

Huang, Y., & Han, M. (2011). The influence of α -Al₂O₃ addition on microstructure, mechanical and formaldehyde adsorption properties of fly ash-based geopolymer products. *Journal of Hazardous Material (193), Science Direct* , 90-94.

Jaan, R. (2012, June 24). *Differences between physisorption and chemisorption*. Retrieved May 16, 2014, from JAAN's Science Class:
<http://jscienceclass.blogspot.com/2012/06/physisorption-and-chemisorption.html>

Kim, M.-J., & Chea, G.-H. (2012). Study on the PV Driven Dehumidifying System with Oyster Shell and Thermoelectric Device.

Liu, L. P., Cui, X. M., Qiu, S. H., Yu, J. L., & Zhang, L. (2010). Preparation of phosphoric acid-based porous geopolymers. *Applied Clay Science 50 (2010), Science Direct* , 600-603.

Marangkos, I., Giannopoulou, I. P., & Papias, D. (2009). Synthesis of ferronickel slag-based geopolymers. *Mineral Engineering, Volume 22, Issue 2* , 196-203.

Mastersizer 2000. (n.d.). Retrieved May 24, 2014, from Malvern:
http://www.malvern.com/en/products/product-range/mastersizer-range/mastersizer-2000/default.aspx?utm_source=ask-powtech.de&utm_medium=online%2Badvertising&utm_campaign=mastersizer%2Benglish

Rattanasak, U., & Chindaprasirt, P. (2009). Influence of NaOH solution on the synthesis of fly ash geopolymer. *Minerals Engineering 22,12* , 1073-1078.

Repo, E., Warchol, J. K., Kurniawan, T. A., & Sillanpaa, M. E. (2010). Adsorption of Co(II) and Ni(II) by EDTA- and/or DTPA-modified chitosan: Kinetic and equilibrium modelling. *Chemical Engineering Journal* , 73-82.

Reusch, W. (2013). *Infrared Spectroscopy*. Retrieved July 18, 2014, from -:
<http://www2.chemistry.msu.edu/faculty/reusch/VirtTxtJml/Spectrpy/InfraRed/infrared.htm>

Riessen, A. v., & Tan, N. C. (2013). Beneficiation of Collie fly ash for synthesis of geopolymer: Part 1 – Beneficiation. *Fuel 106* , 569-575.

Sadangi, J. K., Muduli, S. D., Nayak, D. B., & Mishra, P. B. (2013). Effect of Phosphate ions on preparation of fly ash based geopolymer. *IOSR Journal of Applied Science* , 20-26.

Saika, B. J., & Parthasarathy, G. (2010). Fourier Transform Infrared Spectroscopic Characterization of Kaolinite from Assam and Meghalaya, Northeastern India. *J. Mod. Phys., 2010, 1* , 206-210.

Savova, D., Apak, E., Ekinci, E., Yardim, F., Petrov, N., Budinova, T., et al. (2001). Biomass conversion to carbon adsorbents and gas. *Biomass and Bioenergy, ScienceDirect* , 133-142.

Scanning Electron Microscope. (2014). Retrieved April 8, 2014, from Purdue University: Radiological and Environmental Management: <http://www.purdue.edu/rem/rs/sem.htm#3>

Temuujin, J., Minjigmaa, A., Davaabal, B., & Amgalan, J. (n.d.). Characterisation of Granulometric Composition of a Mongolian Fly Ash and Its Application for Value Added Products. *IEEE* .

The Sample Analysis Process. (2001). *Introduction to Fourier Transform Infrared Spectroscopy* . Madison, Wisconsin, U.S.A.: Thermo Nicolet.

Types of Adsorption. (n.d.). Retrieved April 1, 2014, from Classle beta: Learning is Social: <https://www.classle.net/book/types-adsorption>

Vijaya Rangan, B. (2010). Fly Ash-based Geopolymer Concrete. *Proceedings of the International Workshop on Geopolymer Cement and Concrete* , 68-106.

Wen, X., Yang, Q., Yan, Z., & Deng, Q. (2011). Determination of cadmium and copper in water and food samples by dispersive liquid–liquid microextraction combined with UV–vis spectrophotometry. *Microchemical Journal, Vol 97, Issue 2* , 249-254.

What is FT-IR? (2001). *Introduction to Fourier Transform Infrared Spectroscopy* . Madison, Wisconsin, U.S.A.: Thermo Nicolet.

What is geopolymer? Introduction. (2013, Jun 25). Retrieved April 2, 2014, from Geopolymer Institute: <http://www.geopolymer.org/science/introduction>

Wilson, L. (2014, April). *Copper Toxicity Syndrome*. Retrieved May 13, 2014, from http://drlwilson.com/articles/copper_toxicity_syndrome.htm

Zheng, L., Wang, W., & Shi, Y. (2010). The effects of alkaline dosage and Si/Al ratio on the immobilization of heavy metals in municipal solid waste incineration fly ash-based geopolymer. *Chemosphere 79, Science Direct* , 665-671.